

**Consistency of agricultural drought characterization over Upper
Greater Horn of Africa (1982-2013): Topographical, gauge density,
and model forcing influence**

Author

Agutu, Nathan, Awange, Joseph, Ndehedehe, Christopher, Mwaniki, M

Published

2019

Journal Title

Science of the Total Environment

Version

Accepted Manuscript (AM)

DOI

[10.1016/j.scitotenv.2019.135149](https://doi.org/10.1016/j.scitotenv.2019.135149)

Rights statement

© 2019 Elsevier. Licensed under the Creative Commons Attribution-NonCommercial-NoDerivatives 4.0 International Licence (<http://creativecommons.org/licenses/by-nc-nd/4.0/>) which permits unrestricted, non-commercial use, distribution and reproduction in any medium, providing that the work is properly cited.

Downloaded from

<http://hdl.handle.net/10072/389443>

Griffith Research Online

<https://research-repository.griffith.edu.au>

Journal Pre-proofs

Consistency of agricultural drought characterization over Upper Greater Horn of Africa (1982-2013): Topographical, gauge density, and model forcing influence.

N.O. Agutu, J.L. Awange, C. Ndehedehe, M. Mwaniki

PII: S0048-9697(19)35141-1

DOI: <https://doi.org/10.1016/j.scitotenv.2019.135149>

Reference: STOTEN 135149



To appear in: *Science of the Total Environment*

Received Date: 13 June 2019

Accepted Date: 22 October 2019

Please cite this article as: N.O. Agutu, J.L. Awange, C. Ndehedehe, M. Mwaniki, Consistency of agricultural drought characterization over Upper Greater Horn of Africa (1982-2013): Topographical, gauge density, and model forcing influence., *Science of the Total Environment* (2019), doi: <https://doi.org/10.1016/j.scitotenv.2019.135149>

This is a PDF file of an article that has undergone enhancements after acceptance, such as the addition of a cover page and metadata, and formatting for readability, but it is not yet the definitive version of record. This version will undergo additional copyediting, typesetting and review before it is published in its final form, but we are providing this version to give early visibility of the article. Please note that, during the production process, errors may be discovered which could affect the content, and all legal disclaimers that apply to the journal pertain.

© 2019 Published by Elsevier B.V.

1 Consistency of agricultural drought characterization over Upper
2 Greater Horn of Africa (1982-2013): Topographical, gauge density,
3 and model forcing influence.

4 N.O. Agutu^{a,b}, J.L. Awange^{a,c}, C. Ndehedehe^{a,d}, M. Mwaniki^b

5 ^a*School of Earth and Planetary Sciences, Spatial Sciences, Curtin University, Perth, Australia*

6 ^b*Department of Geomatic Engineering and Geospatial Information Systems JKUAT, Nairobi, Kenya*

7 ^c*Geodetic Institute, Karlsruhe Institute of Technology, Engler-Strasse 7, D-76131, Karlsruhe, Germany*

8 ^d*Australian Rivers Institute and Griffith School of Environment & Science, Griffith University, Nathan,
9 Queensland 4111, Australia*

10 **Abstract**

11 The negative impact of Upper Greater Horn of Africa's (UGHA) complex topography
12 on drought characterization exacerbated by gauge density and model forcing parameters has
13 not been investigated. In order to fill this gap, this study employs a combination of re-
14 motely sensed, in-situ, and model products (1982-2013); precipitation (CHIRPS, GPCC, and
15 CHIRP), soil moisture (ERA-Interim, MERRA-2, CPC, GLDAS, and FLDAS), vegetation
16 condition index (VCI), and total water storage products (GRACE and MERRA-2) to (i) char-
17 acterize drought, (ii) explore the inconsistencies in areas under drought due to topographical
18 variations, gauge density, and model forcing parameters, and (iii), assess the effectiveness of
19 various drought indicators over Ethiopia (a selected UGHA region with unique topographical
20 variation). A 3-month time scale that sufficiently captures agricultural drought is employed to
21 provide an indirect link to food security situation in this rain-dependent region. The spatio-
22 temporal drought patterns across all the products are found to be dependent on topography
23 of the region, at the same time, the inconsistencies in characterizing drought is found to be
24 mainly driven by topographical variability (directly) and gauge density (inversely) for pre-
25 cipitation products while for soil moisture products, precipitation forcing parameters plays
26 a major role. In addition, the inconsistencies are found to be higher under extreme and
27 moderate droughts than severe droughts. The mean differences in the percentage of areas

28 under drought and different drought intensities over the region are on average 15.87% and
29 6.16% (from precipitation products) and 12.65% and 5.20% (from soil moisture products),
30 respectively. On the effectiveness of various indicators, for the duration under study, the fol-
31 lowing were found to be most suitable over Ethiopia; VCI, GPCC, ERA, CPC, and FLDAS.
32 These results are critical in putting into perspective drought analysis outcomes from various
33 products.

34 *Keywords:* Agricultural drought, effectiveness of drought indicators, total water storage,
35 VCI, Standardized Index, Standardized Soil Moisture Index.

36 1. Introduction

37 A majority of the population of the Upper Greater Horn of Africa (UGHA; Djibouti,
38 Somalia, Ethiopia, Sudan, Eritrea, and South Sudan) relies heavily on subsistence agriculture,
39 an activity that has been frequently impacted by droughts, leaving the population vulnerable
40 to famine (*Ibrahim, 1988; Olsson, 1993; Gebrehiwot et al., 2011*). Further consequences of
41 drought in UGHA include; population displacement, rise in food prices, malnutrition and
42 health related complications (*Ibrahim, 1988; Edossa et al., 2010; Taffesse et al., 2012; Viste*
43 *et al., 2013*). In addition, due to the fact that agriculture is largely rain-fed in Ethiopia and
44 combination of rain-fed and irrigated in Sudan and Somalia (e.g., *Bewket, 2009; Elagib and*
45 *Elhag, 2011; Longley et al., 2001*), drought occurrence frequently leads to large-scale crop
46 failures and losses of livestock. The magnitude and severity of the drought impacts in the
47 region emphasize the need for drought indicators that provide a clear, accurate, and consistent
48 picture of the drought extent.

49 Several studies have characterized and analysed droughts in the region from meteorological,
50 agricultural to hydrological (see, e.g., *Gedif et al., 2014; Kurnik et al., 2011; Gebrehiwot et al.,*
51 *2011; Edossa et al., 2010; Viste et al., 2013; Lyon, 2014; Nicholson, 2014; Dutra et al., 2013;*
52 *Awange et al., 2016; Anderson et al., 2012*). These studies have analyzed droughts based on
53 soil moisture (model and re-analysis), rainfall (satellite-derived, in-situ, and a combination of
54 both), Gravity Recovery and Climate Experiment (GRACE) terrestrial water storage (TWS),

55 and normalised difference vegetation index (NDVI). Due to the limitations associated with
56 in-situ rainfall (see, e.g., *Naumann et al., 2014; Nicholson, 2014; Rojas et al., 2011*), most of
57 the studies have preferred satellite or satellite - in-situ merged products which provide homo-
58 geneous, consistent, and wide coverage (e.g., *Damberg and AghaKouchak, 2014*). However,
59 these satellite precipitation and the other aforementioned products do have inherent errors
60 and uncertainties, e.g., errors arising from retrieval algorithms, data acquisition and post-
61 processing, estimation from cloud top reflectance, model limitations, and infrequent satellite
62 overpasses (see, e.g., *Rojas et al., 2011; Damberg and AghaKouchak, 2014; Hong et al., 2006;*
63 *Naumann et al., 2014; AghaKouchak et al., 2009*). Even though the above uncertainties can
64 be reduced through standardization (e.g., Standardized Precipitation Index) or percentiles
65 over time (*McNally et al., 2016*), the impacts of UGHA topography on these products and
66 subsequent propagation of these impacts on agricultural drought characterization is largely
67 unknown.

68 The complex terrain-precipitation relationship in the UGHA region, especially over Ethiopia,
69 has been reported in several research (e.g., *Romilly and Gebremichael, 2011; Dinku et al., 2007,*
70 *2008*). Terrain has been found to be a major factor influencing rainfall distribution, and as
71 such, has been a problem to both satellite-derived and gauge gridded (dependent on gauge
72 density and topography) rainfall products. Satellite derived rainfall products employ either in-
73 frared or passive microwave techniques to determine the amount of rainfall (*Dinku et al., 2007,*
74 *2008*), both of which are impacted by topography especially for convective rainfall as is found
75 in the UGHA. Soil moisture being an integration of rainfall anomalies over time (*Sheffield and*
76 *Wood, 2008*) is expected to be influenced by this complex terrain-precipitation relationship.

77 Furthermore, the quality of model/reanalysis soil moisture is majorly influenced by the
78 precipitation product it is forced by, and the individual model characteristics such as differ-
79 ent operating soil wetness thresholds, i.e., differing variances and mean values; and critical
80 hydrological thresholds, e.g., beginning of surface run-off or levels of evaporation at the po-
81 tential rates (*Dirmeyer et al., 2004*). Despite the significant impacts of topography and gauge

82 density on rainfall and soil moisture products, majority of drought studies in the UGHA re-
83 gion (including the aforementioned) using these products have not addressed their impacts on
84 agricultural drought analysis results.

85 The failure of drought studies in the region to analyze and/or incorporate the impacts
86 of topography and/or gauge density on the analysis results could lead to confusion and/or
87 reduced confidence on drought analysis results due to inconsistencies between various indica-
88 tors. These inconsistencies could arise from propagation of varying impacts of topography and
89 gauge density on different products during drought characterization. To this end, this study
90 considers the impacts of *terrain*, *gauge density*, and *model forcings* on agricultural drought
91 analysis using soil moisture, vegetation condition index, rainfall, and terrestrial water storage
92 products over the period 1982 – 2013. Specifically, the study explores (i) spatio-temporal
93 agricultural drought patterns, (ii) the inconsistencies in areas under agricultural drought due
94 to topographical variations, gauge density, and model forcing parameters, and (iii), the ef-
95 fectiveness of various drought indicators in capturing agricultural drought over Ethiopia as
96 evidenced from national annual crops such as maize and wheat. The first two objectives are
97 carried out over the entire UGHA region while the third objective is carried out only over
98 Ethiopia. This is because Sudan, South Sudan, and Somali carry out both rain-fed and ir-
99 rigated agriculture (*Elagib and Elhag, 2011; Larsson, 1996*) and therefore their annual crop
100 production does not tally with natural water changes in the environment as represented by
101 the indicators.

102 The remainder of the study is organized as follows. A brief description of the study area
103 (UGHA) and the data used are presented in Section 2, followed by methodology in Section
104 3. The results and discussion are presented in Section 4 and 5, respectively, and the study
105 concluded in Section 6.

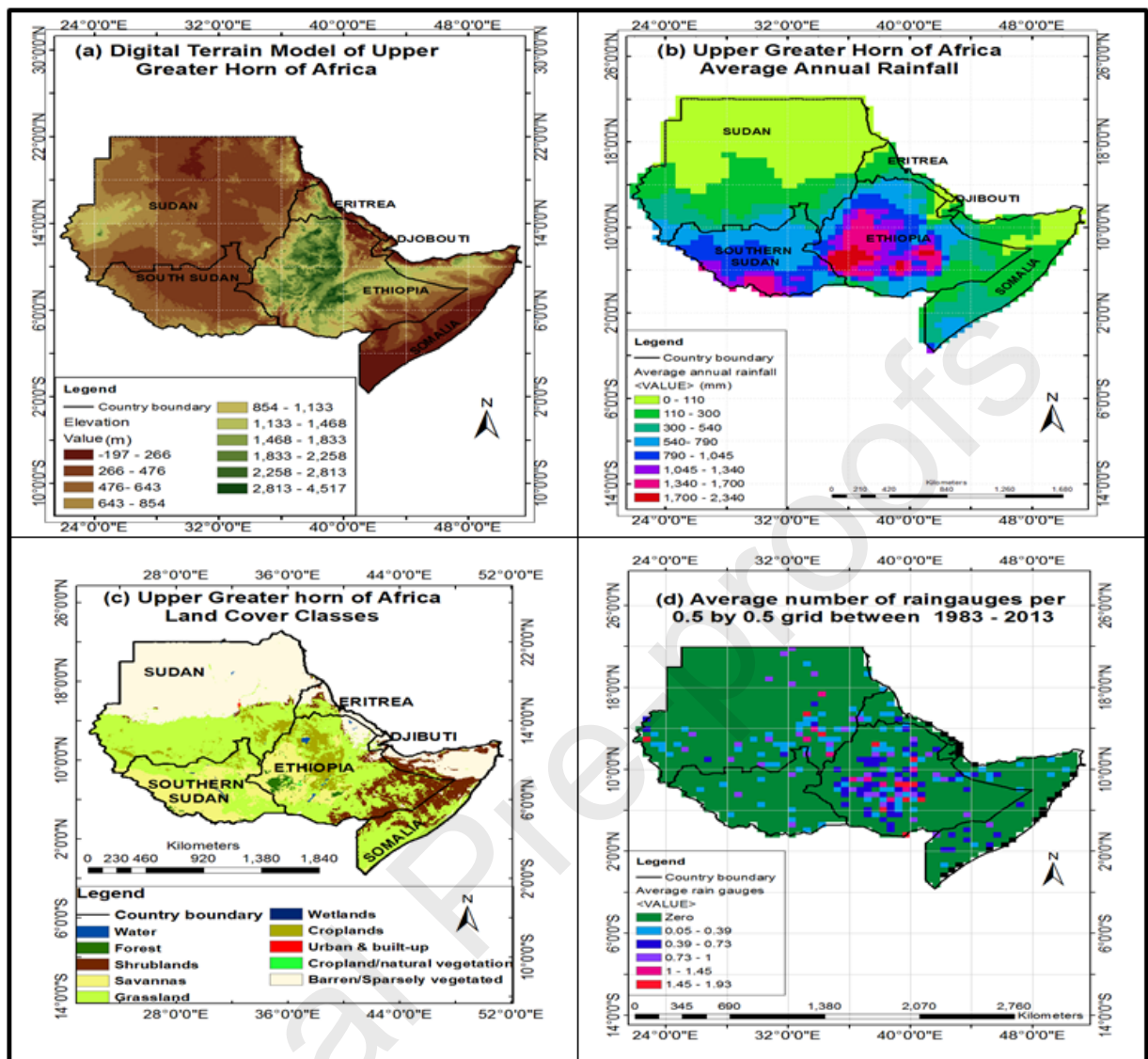


Figure 1: The Upper Greater Horn of Africa (UGHA); (a) Elevation (derived from Shuttle Radar Topographical Mission; SRTM, source:<http://www.cgiar-csi.org/data/srtm-90m-digital-elevation-database>), (b) Average annual rainfall, (c) Land cover types (modified from:<http://e4ftl01.cr.usgs.gov/MOTA/MCD12Q1.051/>), and (d), Average number of rain gauges per 0.5° by 0.5° grids between 1983 - 2013, used in deriving Global Precipitation Climatology Centre (GPCP) rainfall.

2. Study area and data

2.1. Upper Greater Horn of Africa (UGHA)

The UGHA region comprises of Djibouti, Somalia, Ethiopia, Sudan, Eritrea, and South Sudan (Fig. 1). Ethiopia has a complex topography (consisting mostly of high plateaus and chain of mountains) highlighted by the Great Rift Valley, which divides the country roughly along the centre in the northeast to southwest direction (*Romilly and Gebremichael, 2011*). Ethiopian highlands occur on both sides of the Great Rift Valley with the highest elevation on these highlands being in excess of 4500 m (Fig. 1a). The topography on the southeastern side of the highlands descend and levels off towards the border with Somalia (Fig. 1a; *Romilly and Gebremichael, 2011*). Topography plays a major role on Ethiopian climate resulting in a diverse micro-climate ranging from cold highlands to hot desert over southeastern lowlands (*Dinku et al., 2008*). Ethiopia has annual rainfall ranging from over 2000 mm over the highlands to about 300 mm over the low semi-arid lowlands (Fig. 1b), and has seen a rise in frequency of drought from one in every 10 -15 years a century ago to one in every 5 years or less in 2010 (*Edossa et al., 2010*). Sudan and South Sudan consist mostly of flat and/or undulating plains with a south-north gradient (Fig. 1a). It has annual rainfall varying from over 1200 mm in the extreme south west, reducing gradually to approximately 25 mm in the North (*Elagib, 2013*), with climate that varies from equatorial in the southern most parts, savannah in the center, and continental in the north (*Elagib and Elhag, 2011*). Somalia has a weak bimodal rainfall with the main season running from April to July and a second and/or minor season running from September to November (*Longley et al., 2001*). Agriculture is both rain-fed and irrigated with crops are grown during both the main and minor rainfall seasons. The major rain producing feature in the UGHA region is the Inter Tropical Convergence Zone (ITCZ; *Dinku et al. (2008)*). While the climate in the UGHA region is dependent on altitude, the vegetation types mirrors the rainfall zones (see, e.g., Fig. 1b and c; *Kurnik et al., 2011*). The region has relatively high concentration of rain gauges over Ethiopia highlands (Fig. 1d).

132 2.2. Data

133 Table 1 summaries the dataset used in this study.

Table 1: Overview of data-set employed in the study

Data	Temporal resolution	Spatial resolution	Period employed	References/ Studies used in	
Precipitation	CHIRPS	Monthly	0.05° × 0.05°	1982 - 2013	<i>Funk et al. (2015)</i> ; <i>Pricope et al. (2013)</i> ; <i>Shukla et al. (2014)</i> ; <i>(McNally et al., 2016)</i> .
	CHIRP	Monthly	0.05° × 0.05°	1982 - 2013	<i>Funk et al. (2015)</i> .
	GPCC	Monthly	0.5° × 0.5°	1982 - 2013	<i>Schneider et al. (2014)</i> ; <i>Kurnik et al. (2011)</i> ; <i>Funk et al. (2014)</i> ; <i>Ziese et al. (2014)</i> ; <i>Dutra et al. (2014)</i> .
Soil moisture	MERRA-2	Monthly	0.625° × 0.5°	1982 - 2013	<i>Bosilovich et al. (2016, 2015)</i> .
	GLDAS	Monthly	1° × 1°	1982 - 2013	<i>Rodell et al. (2004)</i> ; <i>Anderson et al. (2012)</i> ; <i>Yilmaz et al. (2014)</i> ; <i>McNally et al. (2016)</i> .
	ERA-Interim	Monthly	0.25° × 0.25°	1982 - 2013	<i>Albergel et al. (2012)</i> ; <i>Balsamo et al. (2009)</i> ; <i>Dee et al. (2011)</i> ; <i>Decker et al. (2012)</i> ; <i>Dutra et al. (2013)</i> ; <i>Viste et al. (2013)</i> .
	FLDAS VIC	Monthly	0.25° × 0.25°	1982 - 2013	<i>Rui and McNally (2016)</i> ; <i>McNally et al. (2017)</i> ; <i>Yilmaz et al. (2014)</i> ; <i>Agutu et al. (2017)</i> .
	FLDAS Noah	Monthly	0.1° × 0.1°	1982 - 2013	<i>Yilmaz et al. (2014)</i> ; <i>McNally et al. (2017)</i> ; <i>Rui and McNally (2016)</i> ; <i>Agutu et al. (2017)</i> .
	CPC	Monthly	0.5° × 0.5°	1982 - 2013	<i>van den Dool et al. (2003)</i> ; <i>Dirmeyer et al. (2004)</i> ; <i>Fan and van den Dool (2004)</i> .
VCI	NDVI	15 days	5-arc-minute	1982 - 2013	<i>Verdin et al. (2005)</i> ; <i>Pinzon and Tucker (2014)</i> ;
					<i>Tucker et al. (2005)</i> ; <i>Rojas et al. (2011)</i> ; <i>Guan et al. (2012)</i> ; <i>Dorigo et al. (2012)</i> ; <i>Chen et al. (2014)</i> .
TWS	GRACE	Monthly	1° × 1°	2003 - 2013	<i>Long et al. (2013)</i> ; <i>Wouters et al. (2014)</i> ; <i>Awange et al. (2016)</i> ; <i>Chen et al. (2009)</i> ; <i>Tapley et al. (2004)</i> ; <i>Chen et al. (2004)</i> .
	MERRA-2	Monthly	0.625° × 0.5°	1982 - 2013	<i>Bosilovich et al. (2016, 2015)</i> .

134 2.2.1. Rainfall Products

135 Climate Hazard Group InfraRed Precipitation with Stations (CHIRPS) monthly 0.05°
 136 version 2 precipitation (1982–2013) obtained from [ftp://ftp.chg.ucsb.edu/pub/org/chg/
 137 products/CHIRPS-2.0/](ftp://ftp.chg.ucsb.edu/pub/org/chg/products/CHIRPS-2.0/) is used. It is a combination of in-situ gauge and satellite-based cold
 138 cloud duration (CCD) observations (see *Funk et al. (2015)* for more details).

139 In addition, Climate Hazard Group InfraRed Precipitation(CHIRP), a satellite only prod-
140 uct based on CCD observations is used. The monthly 0.05° , precipitation (1982–2013) ob-
141 tained from <ftp://ftp.chg.ucsb.edu/pub/org/chg/products/CHIRP/> was used to charac-
142 terize drought (see, *Funk et al., 2015*, for more details).

143 Finally, Global Precipitation Climatology Centre (GPCC) (*Schneider et al., 2014*) monthly
144 0.5° version 7 precipitation for the duration 1982 – 2013 from [ftp://ftp.dwd.de/pub/data/](ftp://ftp.dwd.de/pub/data/gpcc/html/fulldata_v7_doi_download.html)
145 [gpcc/html/fulldata_v7_doi_download.html](ftp://ftp.dwd.de/pub/data/gpcc/html/fulldata_v7_doi_download.html) is also used.

146 2.2.2. Soil moisture products

147 Due to the complex terrain and high rainfall variability in the region, major soil moisture
148 products (model and re-analysis) are used for agricultural drought analysis/characterization
149 in order to decipher and compare the impacts of terrain on agricultural drought characteri-
150 zation consistency using these products. For MERRA-2 (second Modern-Era Retrospective
151 analysis for Research and Applications), root zone soil moisture product was used while for
152 ERA-Interim (European Centre for Medium-Range Weather Forecasts Interim Re-Analysis),
153 FLDAS (Famine Early Warning System Network (FEWS NET) Land Data Assimilation Sys-
154 tem), and GLDAS (Global Land Data Assimilation System), individual soil moisture layers
155 from 0 – 1 m (approximately equal to root zone depth) are aggregated, and CPC (Climate
156 Prediction Center) used the way it is since it is a single depth bucket product.

157 ERA-Interim monthly soil moisture for the duration 1982 – 2013, at 0.25° spatial (grid) res-
158 olution obtained from <http://apps.ecmwf.int/datasets/data/interim-full-moda/levtype=sfc/>
159 is used.

160 MERRA-2, an upgraded version of the MERRA reanalysis (*Rienecker et al., 2011; Decker*
161 *et al., 2012*) employing Goddard Earth Observing System Model, version 5.12.4 (GEOS 5.12.4)
162 data assimilation system (*Bosilovich et al., 2016*), is used. The monthly root zone soil moisture
163 at spatial resolution of 0.625° by 0.5° , for the duration 1982–2013 was downloaded from
164 https://gmao.gsfc.nasa.gov/reanalysis/MERRA-2/data_access/.

165 GLDAS (*Rodell et al., 2004*) NOAA-model variant, version 2, is used. The 1° by 1°

166 monthly soil moisture for the period 1982 – 2010 was obtained from [http://disc.sci.gsfc.](http://disc.sci.gsfc.nasa.gov/\services/grads-gds/gldas)
167 [nasa.gov/\services/grads-gds/gldas](http://disc.sci.gsfc.nasa.gov/\services/grads-gds/gldas). Like ERA-Interim’s case, GLDAS moisture layers
168 (0 – 1 m) are aggregated before agricultural drought analysis. The Noah model variant has
169 been used widely by the atmospheric and modeling communities thus model parameters are
170 adequately tested (*McNally et al., 2016*). Besides (*McNally et al., 2016*), several studies (e.g.,
171 *Yilmaz et al., 2014; Anderson et al., 2012*) have used the model over the region.

172 FLDAS (*McNally et al., 2017; Rui and McNally, 2016*), Noah and VIC model variants at
173 0.1° by 0.1° , and 0.25° by 0.25° spatial resolutions, respectively, are used. The monthly soil
174 moisture for the duration 1982 – 2013 was obtained from [https://ldas.gsfc.nasa.gov/](https://ldas.gsfc.nasa.gov/FLDAS/FLDASdownload.php)
175 [\FLDAS/FLDASdownload.php](https://ldas.gsfc.nasa.gov/FLDAS/FLDASdownload.php). The Noah and VIC moisture products are from FLDAS simu-
176 lation run forced by CHIRPS precipitation, and soil moisture and state fields from MERRA-2.
177 It has been used in the region by several studies, (e.g., *McNally et al., 2016; Yilmaz et al.,*
178 *2014; Agutu et al., 2017; Anderson et al., 2012*), among others.

179 Finally, Climate Prediction Center (CPC, *van den Dool et al. (2003)* and *Fan and van den*
180 *Dool (2004)*) global, version 2 soil moisture is used. The monthly 0.5° by 0.5° spatial resolution
181 mean soil moisture, from 1982 to 2013 was downloaded from NOAA’s Earth System Research
182 Laboratory (<http://www.esrl.noaa.gov/psd/data/gridded/data.cpcsoil.html>).

183 2.2.3. Total water storage (TWS)

184 The Centre for Space Research’s (CSR) release five (RL05) monthly GRACE (see, e.g.,
185 *Wouters et al., 2014; Tapley et al., 2004*) spherical harmonic coefficients for the duration 2003
186 — 2013 obtained from <http://icgem.gfz-potsdam.de/ICGEM/shms/monthly/csr-rl05/> are
187 used in this study. The spherical harmonic coefficients are processed following *Wahr et al.*
188 (*1998*) and detailed description of the processing can be found in *Agutu et al. (2017)*.

189 The resulting GRACE-derived TWS over upper GHA comprises changes from biomass/canopy
190 water content (assumed to be negligible), surface water, accumulated soil moisture, and
191 groundwater. The surface water variations corresponding to Lake Tana (dominant water
192 body in the region) was removed through integration of satellite altimetry lake level changes

193 and lake Kernel function following *Moore and Williams* (2014). Assuming the contribution of
194 other surface water bodies in the region, e.g., from the Sudd wetland to be negligible, the re-
195 moval of the dominant Lake Tana's surface contribution enabled the remaining TWS changes
196 to be associated with groundwater and soil moisture. Further, due to shorter duration under
197 consideration and limited exploitation of groundwater in the region, most of the variation
198 is assumed to occur in the unsaturated zone (soil moisture) as it responds more to climate
199 variability than the saturated zone (e.g., *Yang et al.*, 2014). The remaining components is
200 henceforth referred to as GTWS. Its utility in drought and hydrology related analyses has
201 been demonstrated in a number of research (see, e.g., *Awange et al.*, 2016; *Long et al.*, 2013;
202 *Chen et al.*, 2009).

203 In addition, MERRA-2 Monthly 0.5° by 0.625° (spatial resolution) total land water storage
204 (TWLAND) for the duration 1982 – 2013 obtained from [https://gmao.gsfc.nasa.gov/
205 reanalysis/\MERRA-2/data_access/](https://gmao.gsfc.nasa.gov/reanalysis/\MERRA-2/data_access/) is also employed. It is hereafter referred to as MTWS.
206 Unlike GTWS, MTWS does not contain groundwater and canopy water content (see, e.g.,
207 *Reichle*, 2012)

208 2.2.4. Vegetation Condition Index (VCI)

209 National Oceanic and Atmospheric Administration's Advanced Very High-Resolution Ra-
210 diometer (AVHRR) long term series NDVI data set (see, e.g., *Pinzon and Tucker*, 2014;
211 *Tucker et al.*, 2005) from 1982-2013, 15 days composite at $\simeq 0.0833^\circ$ (8 km) spatial resolu-
212 tion obtained from <http://ecocast.arc.nasa.gov/data/pub/\gimms/3g.v0/> is utilized in
213 computing VCI (*Kogan*, 1995). VCI is preferred for agricultural drought analysis due to its
214 ability to isolate and/or emphasize weather related vegetation stress (see, e.g., *Rojas et al.*,
215 2011; *Quiring and Ganesh*, 2010; *Kogan*, 1995) that correspond to water availability within
216 the study area. It was computed following (*Kogan*, 1995) and (*Agutu et al.*, 2017). AVHRR
217 NDVI has been used extensively globally and over Africa for drought and other related stud-
218 ies (see, e.g., *Chen et al.*, 2014; *Dorigo et al.*, 2012; *Rojas et al.*, 2011; *Guan et al.*, 2012;
219 *Verdin et al.*, 2005).

220 2.2.5. National annual crop production

221 The national annual crop (maize and wheat) production data for Ethiopia obtained from
222 Food and Agriculture Organization (FAO) data portal ([http://www.fao.org/faostat/en/](http://www.fao.org/faostat/en/#data/QC)
223 [#data/QC](http://www.fao.org/faostat/en/#data/QC)) is employed in evaluating how well the various drought indices capture agricultural
224 droughts.

225 3. Methodology

226 A Standardised Index (e.g., Standardised Precipitation Index, *McKee et al., 1993*) is em-
227 ployed to characterize agricultural drought using Rainfall (CHIRPS, CHIRP, and GPCC), soil
228 moisture (MERRA, CPC, ERA-Interim, GLDAS, and FLDAS), and TWS (MERRA-derived).
229 In addition, standardized anomalies (SA, *Wu et al., 2001*) is used to characterize agricultural
230 drought using GRACE-derived TWS since its (GRACE-derived TWS) length is too short to fit
231 SPI. Both standardizations are carried out for 3-month time scales since 3-months time scale
232 SPI has been associated with agricultural drought in several research efforts (see, e.g., *Rouault*
233 *and Richard, 2003*; *Kurnik et al., 2011*; *Svoboda et al., 2012*; *Elagib, 2013*). The SI/SA are
234 then decomposed through rotated principal component analysis for spatio-temporal drought
235 patterns. All the products other than GLDAS and GRACE TWS are resampled to 1° by 1°
236 spatial resolution before standardization.

237 3.1. Agricultural Drought Characterization

238 3.1.1. Standardized Index (SI)

239 Standardised precipitation index (SPI, *McKee et al. (1993)*) is a form of standardisation in
240 which precipitation is expressed in terms of its deviation from the long-term mean. It is com-
241 puted by fitting a parametric distribution to precipitation data then transforming parametric
242 distribution function to the standard normal distribution with a mean of 0 and standard de-
243 viation of 1 (see, e.g., *Naresh Kumar et al., 2009*; *Farahmand and AghaKouchak, 2015*). It
244 is one of the most preferred drought indices due to its standardised nature, simplicity (only
245 requires one input), and flexibility of use on different time scales e.g., 1, 3, 6, 9, 12-month (see,

246 e.g., *Svoboda et al., 2012; AghaKouchak, 2015*, and the references therein). A non-parametric
 247 approach of fitting SPI (see, e.g., *AghaKouchak, 2015*) is adopted due to the dependence of the
 248 SPI values on the choice of parametric distribution employed, especially at the tail end of the
 249 distribution (see e.g., *Quiring, 2009*). This approach involves the use of empirical Gringorten
 250 plotting position formula to compute empirical probability, $p(x)$, (*Gringorten, 1963*) as

$$p(x_i) = \frac{i - 0.44}{n + 0.12}, \quad (1)$$

251 where $p(x_i)$ is the empirical probability, n the sample size, and i denotes the rank of non-zero
 252 precipitation data from the smallest. The empirical probability from eqn. 1 is then transformed
 253 into a standardized index as

$$SI = \phi^{-1}(p), \quad (2)$$

254 where SI is SPI, SSI (standardised soil moisture index), SVCI (standardised vegetation con-
 255 dition index), or STWSI (standardised total water storage index) depending on the variable
 256 under consideration, ϕ is the standard normal distribution function, and p is the proba-
 257 bility derived from Eqn. 1. This study employed Standardized Drought Analysis Toolbox
 258 (SDAT, *Farahmand and AghaKouchak (2015)*) in computing SPI values and adopted the SPI
 259 drought limit categories of *Agnew (2000)* in Table 2. For this study, a drought episode be-
 260 gins any time SPI is continuously less than -0.84 for a period of at least three months, and
 261 ends when SPI value exceeds -0.84 . The various drought intensities (moderate, severe, and
 262 extreme) are then said to occur when the values in Table 2 are attained.

263 3.1.2. Standardized Anomalies (SA)

264 SA (*Wu et al., 2001*), also referred to as z-scores, is a form of standardization in which
 265 a variable is expressed in terms of its deviation from its long term mean. It is computed by
 266 dividing the monthly anomalies by the multi-year standard deviation (see, e.g., *Peters et al.,*
 267 *2002; Agutu et al., 2017*, for formulation). It has been applied to study droughts in various
 268 studies (e.g., *Wu et al., 2001; Agnew and Chappell, 1999; Lough, 1997; Katz and Glantz,*

Table 2: Drought intensities as per SPI values (*Agnew, 2000*)

SPI	Drought Category
>1.65	extremely wet
>1.28	severely wet
>0.84	moderately wet
>- 0.84 and <0.84	normal
<-0.84	moderate drought
<-1.28	severe drought
<-1.65	extreme drought

1986). Due to the short duration of GTWS, which does not permit standardization using SPI approach, the 3-month time series of GTWS is standardised using z-scores. The 3-month time series cumulation is computed in a manner similar to SPI cumulations e.g., 3-month time series for January would involve summing from November of the previous year. Positive Z-score values represent wet conditions, zero values represent normal conditions, while negatively values represent dry conditions (*Wu et al., 2001*).

3.1.3. Principal Component Analysis (PCA)

PCA (*Jolliffe, 2002; Preisendorfer, 1988; Wilks, 2006; Lorenz, 1956*) has been used to study the spatio-temporal drought variability in various regions across the world (see., e.g., *Santos et al., 2010; Raziei et al., 2009; Sigdel and Ikeda, 2010*) through the decomposition of spatio-temporal fields, e.g., SPI, SSI, STWSI, SVCI etc. into spatial and corresponding temporal patterns. For formulation, see e.g., *Jennrich (1970); Kutzbach (1967); Hannachi et al. (2006); von Storch and Zwiers (1999)*.

The significant PCA decomposed SI/SA components (based on log-eigenvalue diagrams; *Jolliffe, 2002*) are further subjected Varimax rotation (*Jolliffe, 1995; Kaiser, 1958; Forina et al., 1988*) in order to spread the variance explained and improve interpretability. In addition, the rotation has served to localize the results from regional (GHA) to local (country) level.

286 The resulting spatial pattern, called the scores, properly normalized represents the correlation
 287 (relationship) between the SI/SA and the rotated principal components (RPC) while the
 288 normalized RPC represents the SI/SA (see, e.g., *Bordi et al., 2006*).

289 3.2. Percentage of Areas Under Agricultural Drought and their Consistencies

290 The percentage of areas under agricultural drought and different drought intensities are
 291 evaluated for Ethiopia, Sudan, South Sudan, and Somalia through determination of the per-
 292 centage of pixels under various agricultural drought categories following Table 2. Differences
 293 in percentage areas under agricultural drought and different drought intensities between var-
 294 ious products during 1983 – 1984, 1987, 1999, 2009, and 2010 – 2011 drought events are then
 295 evaluated for each country.

296 In order to evaluate the impact of gauge density, the differences between CHIRPS and
 297 GPCC derived percentages of areas under drought are evaluated (Eqn 3). The in-situ stations
 298 in CHIRPS (global historical networks and global teleconnection networks) are all in GPCC
 299 plus other more stations (see, *Schneider et al., 2014; Funk et al., 2015*), though the number
 300 of stations available on monthly basis differs hence the variations in areas under drought. For
 301 the mean differences due to topography, the following differences are evaluated

$$CHIRPS_{(\% \text{ area under drought})} - GPCC_{(\% \text{ area under drought})} = \text{Influence of gauge density} \quad (3)$$

$$CHIRP_{(\% \text{ area under drought})} - CHIRPS_{(\% \text{ area under drought})} - \text{Influence of gauge density} \\ = \text{Influence of topography} \quad (4)$$

302 Equation 4 arises from the fact that CHIRP, a satellite only product, determines pre-
 303 cipitation from cold cloud duration (CCD; *Funk et al. (2015)*) and the regional topography
 304 has been known to greatly hamper the satellite products (*Romilly and Gebremichael, 2011;*
 305 *Dinku et al., 2007, 2008*). CHIRPS on the other hand has gauge derived rainfall estimates in
 306 addition to CCD estimates; the inclusion of gauge derived estimates serve to correct/scale the

307 CCD estimates to their proper values. This implies that the difference between CHIRPS and
308 CHIRP contain the influence of both gauge and topography.

309 In addition, the following differences are evaluated for soil moisture products; FLDASN
310 (FLDAS NOAH) – FLDASV (FLDAS VIC), FLDASN – MERRA2, MERRA2 – ERA, and
311 FLDASN – GLDAS. The differences between the soil moisture products are taken to explore
312 issues related to the role of forcing precipitation vis-a-vis model differences among other factors
313 in contributing to the inconsistencies in areas under agricultural drought.

314 These differences are then analyzed using ANOVA and Bonferroni multiple comparison
315 methods, for further details see *Kutner (2005)*; *King (2010)* and *Hochberg and Tamhane*
316 *(1987)*; *Toothaker (1993)*, respectively. The analyses are used to explore how the following
317 factors contribute to the differences in percentages of areas under agricultural drought across
318 the region; (i) gauge density, (ii) physical characteristics (topography of each country), (iii)
319 products (rainfall vis-a-vis moisture; different rainfall and soil moisture products), and (iv)
320 forcing precipitation and model types.

321 *3.3. Evaluating the Effectiveness of Various Drought Indicators over Ethiopia*

322 As the national annual crop production is given at country level, the SI/SA (only) over
323 Ethiopia are decomposed through rotated principal component analyses. Then the temporal
324 SI/SA values are extracted and regressed through partial least squares regression (PLSR; for
325 further details, see *Geladi and Kowalski, 1986*; *Wold et al., 2001*) on national annual crop
326 production data (maize/wheat). Detailed explanation of this process can be found in *Agutu*
327 *et al. (2017)*. The evaluation is carried out at 1, 3, and 6 month SI/SA time scales.

328 **4. Results**

329 Long term dataset (rainfall, moisture, vegetation condition index, and MTWS) are stan-
330 dardised following SPI, while GTWS is standardised using Z-score. The resulting standardised
331 variables are regionalised through rotated principal component analysis in order to provide
332 spatio-temporal agricultural drought patterns. In addition, the percentage of areas affected by

333 agricultural droughts are analysed and the consistency of percentage of areas under drought
334 as influenced by terrain, gauge density, and soil moisture model related parameters explored
335 across the region. Finally, the effectiveness of various drought indicators are analyzed over
336 Ethiopia. Only Ethiopia is considered since it is the only country in UGHA practicing rain-fed
337 agriculture hence there is a link between crop production and drought indicators. The other
338 countries do both rain-fed and irrigated agriculture.

339 *4.1. Agricultural Drought Characterization*

340 The regionalization of SI/SA through rotated principal component analysis results in 4
341 largely consistent and significant spatio-temporal patterns across majority of the agricultural
342 drought indicators (Figs. 2 - 5). The geographical coverage of these spatial, from RPCA
343 clustering of SI/SA values, based on Fig. 2 is summarised in Table 3. When assessed in
344 relation to Figure 1, the spatial patterns of the precipitation products (i.e., CHIRPS, CHIRP,
345 and GPCC) are largely similar over the regions and follows the region's topography, while those
346 of VCI and MTWS largely follow land cover classes, and GTWS patterns follow both rainfall
347 and land cover classes (Fig. 2, compared to Fig. 1a-c). All the products show consistent
348 patterns over Region 3, a region of relatively lowland flat topography with low-moderate
349 rainfall (see, Fig. 1a and b). For the soil moisture products, the spatial patterns roughly
350 resemble those of rainfall and/or land cover patterns except for CPC spatial patterns (Fig. 3,
351 compared to Fig. 1b and c). Also, Region 4's spatial patterns are different across the soil
352 moisture products (Fig. 4), with MERRA2's spatial pattern resembling that of MTWS in
353 Region 4 (Fig. 3). Similar to the patterns of the rainfall group (Fig. 3), there is consistency
354 among the soil moisture products over Region 3 (i.e., lowland region of low to moderate
355 rainfall) though not as close as in the rainfall group.

356 The proportion of variances of the SI/SA explained by these components is tabulated in
357 Table 4. The majority of the rainfall products had the lowest variability in Region 4 while the
358 majority of the soil moisture products had the lowest variability in Region 3. Region 4, from
359 rainfall products, comprises mostly Ethiopian highlands; a region with lots of rainfall most of

Table 3: Approximate geographical coverage of SI/SA spatial patterns, based on Fig. 2.

Region	Countries/areas
1	Sudan
2	South Sudan
3	Eastern Ethiopia and Somalia
4	Ethiopian highlands

360 the year hence low variability in SPI while Regions 3 comprises relatively dry regions with low
 361 soil moisture most of the year hence lowest variability in SSI. On the other hand, maximum
 362 variability as seen in Table 4 differed across products with no clear majority in any particular
 363 region. VCI had Regions 1 and 3 explaining equal magnitudes of variability probably due to
 364 similar vegetation types in the vast areas of the two locations (Fig. 2 vis-a-vis Fig. 1c). On the
 365 basis of the total variabilities explained, CHIRPS and GPCC are almost equal but lower than
 366 CHIRP while the soil moisture products fall into 3 categories i.e., FLDASV (43%); GLDAS,
 367 ERA-Interim, and FLDASN (50 – 55%); and CPC and MERRA2 (66 – 67%), see Table 4.

Table 4: Proportions (%) of variances explained in each Region by each spatial pattern. Regions are as shown in Figures 2 and 3.

Region	CHIRPS	CHIRP	GPCC	VCI	MERRA TWS	GRACE TWS	ERA- Interim	GLDAS	CPC	MERRA2	FLDASN	FLDASV
Region 1	10.03	15.78	13.68	8.08	17.50	14.28	15.84	9.95	30.47	18.01	17.53	13.85
Region 2	10.16	8.86	8.41	12.07	20.45	24.35	12.72	15.97	17.52	19.70	10.66	11.27
Region 3	11.38	11.10	11.00	8.05	12.66	23.34	10.91	10.39	8.56	13.20	12.06	10.81
Region 4	8.73	11.81	8.21	10.74	14.52	21.32	16.23	14.44	10.71	15.22	11.93	7.09
Total	40.03	47.55	41.3	38.94	65.13	83.29	55.70	50.75	67.26	66.13	52.18	43.02

FLDASN - FLDAS NOAH, and FLDASV - FLDAS VIC.

368 The SI/SA temporal evolutions show region-wide agricultural drought events in the years
 369 1983/1985, 1986/1987, 1990/1991, 2000, 2005/2006, 2009/2010, and 2010/2011 (see Figs. 4 and 5).

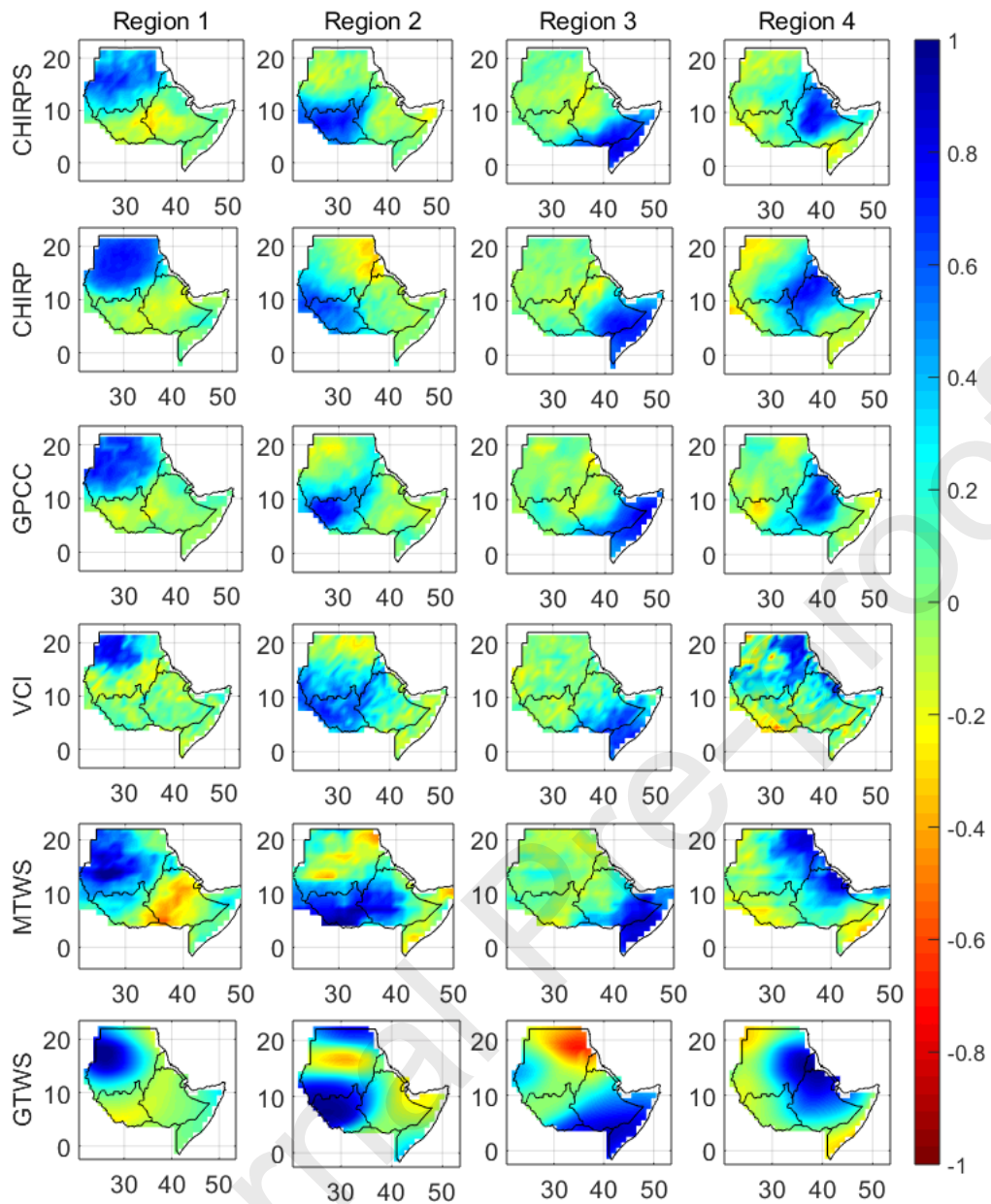


Figure 2: Standardized Indices/Anomalies (SI/SA) spatial patterns. The patterns result from rotated principal component analyses decomposition of SI/SA. They are interpreted jointly with Figure 4, and represent agricultural drought spatial extents whenever Figure 4 falls below -0.84 , as in Table 2, continuously for at least three months. Rows and columns represent drought indicators and regions, respectively. (Y-axis are latitudes and x-axis longitudes).

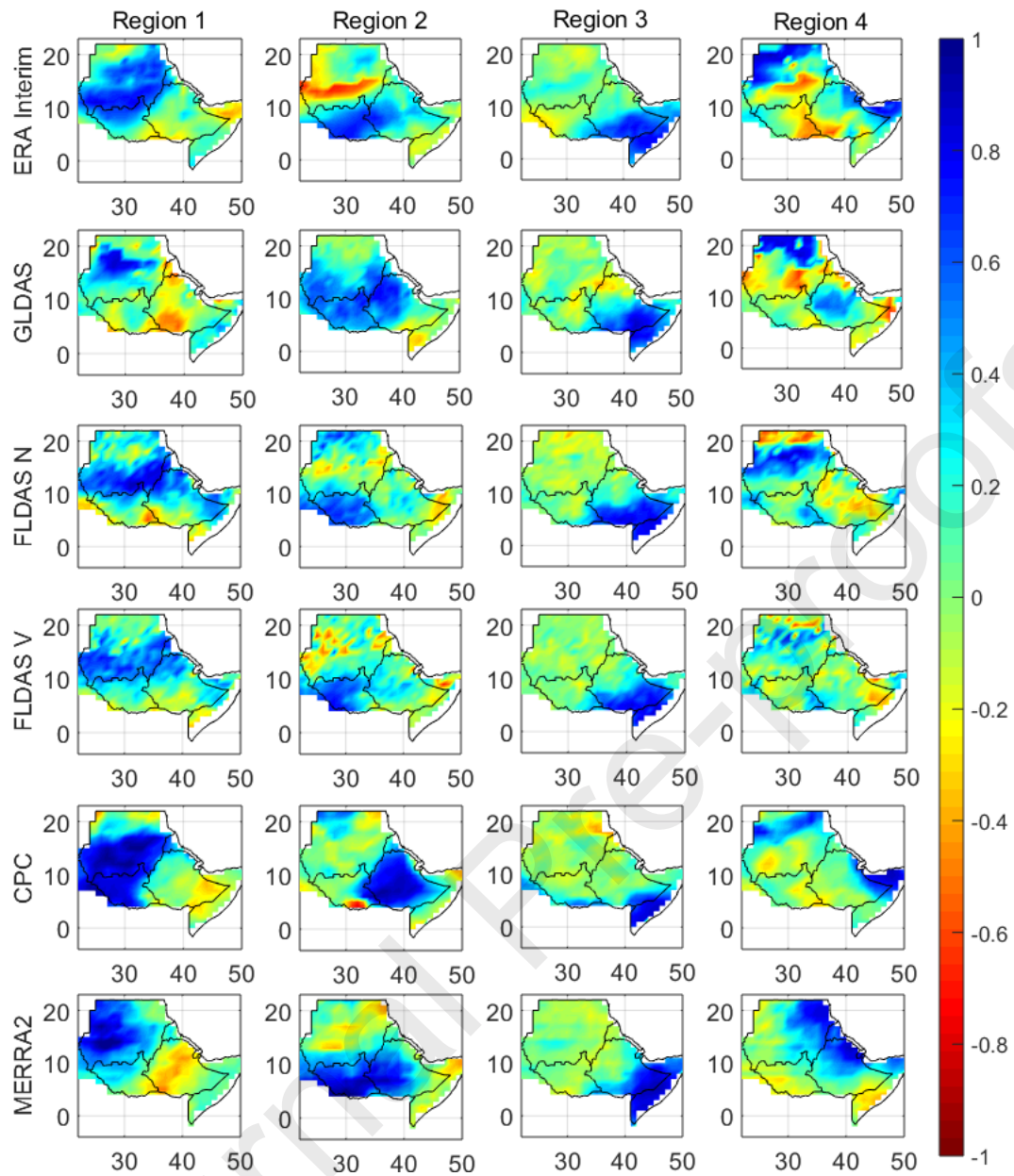


Figure 3: Standardized Indices/Anomalies (SI/SA) spatial patterns. The patterns result from rotated principal component analyses decomposition of SI/SA. They are interpreted jointly with Figure 5 and represent agricultural drought spatial extents whenever Figure 5 falls below -0.84 , as in Table 2, continuously for at least three months. Rows and columns represent drought indicators and regions, respectively. (Y-axis are latitudes and x-axis longitudes).

370 These drought episodes and others showed in the figures are consistent with what is reported
371 by previous studies across GHA (e.g., *Gebrehiwot et al., 2011*; *Elagib and Elhag, 2011*; *Viste*
372 *et al., 2013*; *Nicholson, 2014*; *Williams and Funk, 2011*; *Masih et al., 2014*).

373 Of the precipitation products, GPCC and CHIRPS are similar across all the regions with
374 little differences evident in Regions 1 and 2 (Fig. 4a and b) though they are significantly
375 different from CHIRP across the region (Fig. 4). This could be attributed to both CHIRPS
376 and GPCC containing in-situ rainfall (rain gauge products) while CHIRP is wholly satellite
377 derived hence differences depends on how well these products estimate rainfall across the
378 region, which is a function of topographical changes (see, e.g., *Dinku et al., 2007*; *Romilly*
379 *and Gebremichael, 2011*; *Dinku et al., 2008*). Also, FLDASN and FLDASV are largely close
380 across the whole region (Fig. 5).

381 Over the duration considered, all the indicators are found to be consistent in Region 3
382 more than the rest of the UGHA regions (Figs. 4 and 5), a pattern that is also noticeable in
383 the spatial maps (Figs. 2 and 3). This could be attributed to the facts that this region, a
384 relatively flat region with moderate rainfall (Fig. 1a and b) does not have much topographical
385 influence on the products as compared to high rainfall/rapid terrain changing regions like
386 Region 4 (Fig. 2) and Region 2 (Fig. 3). The satellite and model-based products seems to work
387 consistently well under flat topography and lower rainfall ranges while GPCC interpolation
388 also seems to be good. The soil moisture products are mostly different in Region 2 (Fig. 3
389 and Fig. 5b), which could be attributed to the failure of the models to capture the complex
390 topography-rainfall relationship in the region. Also, the large difference between the temporal
391 evolutions across the soil moisture-based indicators compared to the rainfall indicators could
392 be a pointer to greater inconsistency in the drought information as represented by the soil
393 moisture based indicators. Region 4 of SSI (Fig. 5) represent the region with the largest
394 difference in temporal evolution possibly due to different spatial patterns as observed from
395 the spatial SSI patterns (Fig. 3).

396 In general, some isolated performances are also observed from MTWS and GLDAS. MTWS

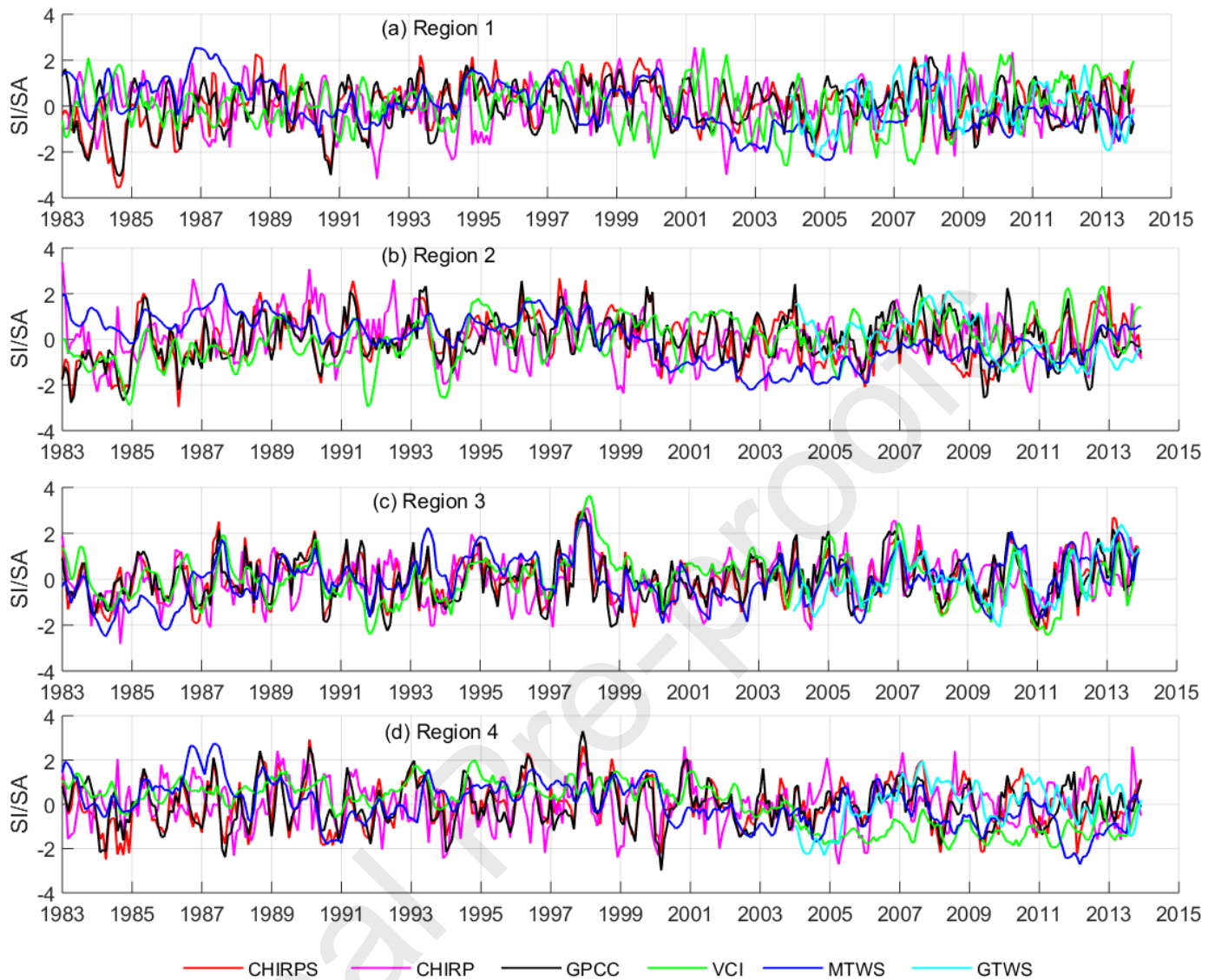


Figure 4: Standardized Indices/Anomalies (SI/SA) temporal evolution. They are the corresponding temporal evolution of spatial patterns in Fig. 2, from rotated principal component analyses decomposition of SI/SA. Agricultural drought conditions occur when SI/SA falls below -0.84 , as in Table 2, continuously for at least three months. (Y-axis values are unitless).

397 appears to have a shift with pre-1999 being predominantly wet and dry afterward (Fig. 4a
 398 and b), while GLDAS appears to have issues in Regions 2 and 4 though consistent with other
 399 products in Region 3 (Fig. 5). Also, CPC and MERRA2 are closer over the region. Further,

400 there is a lag in drought events from rainfall to VCI/soil moisture followed by MTWS and
 401 eventually GTWS.

402 Finally, the relationships between the temporal patterns of the SI/SA (Figs. 4 and 5) ana-

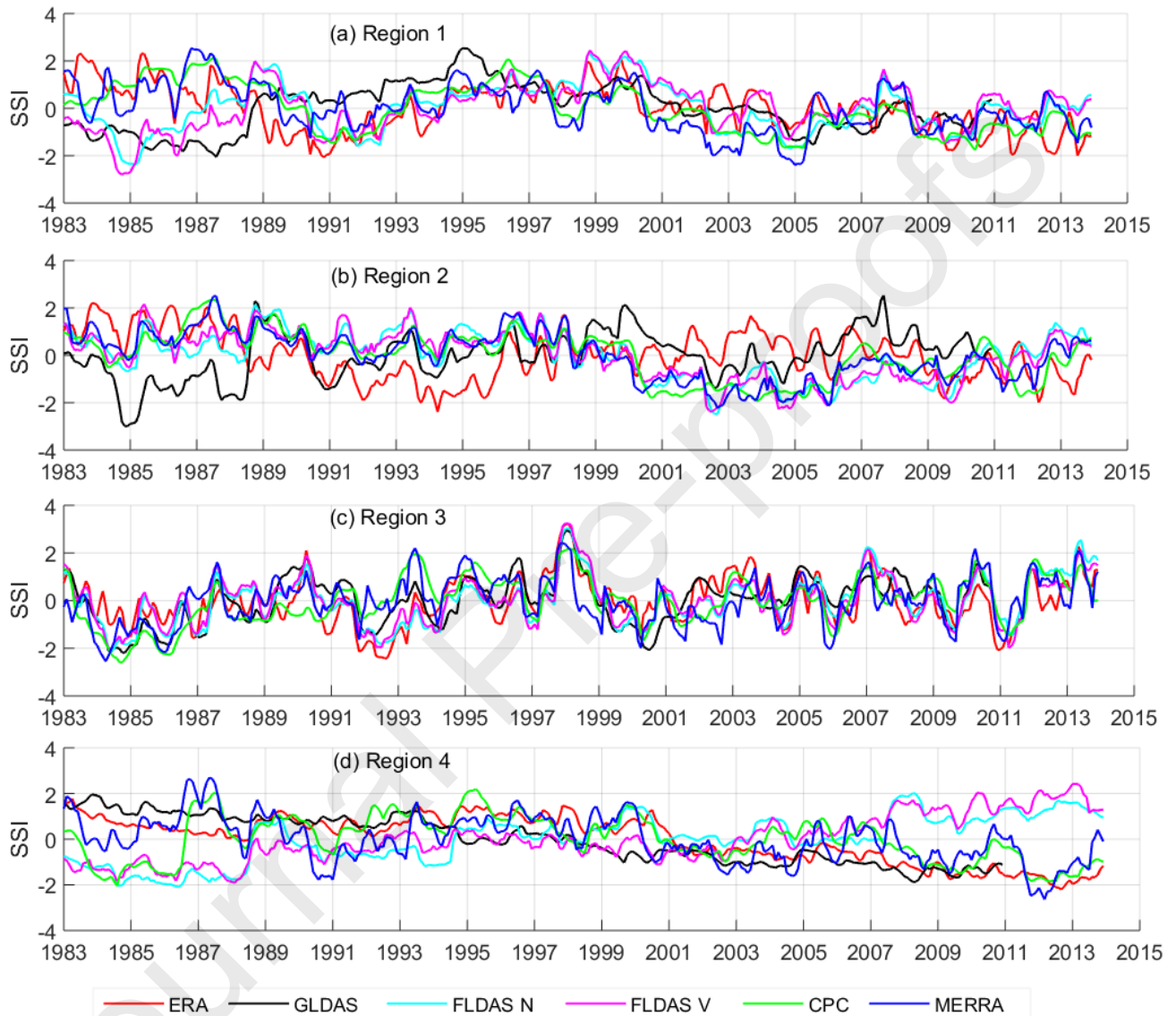


Figure 5: Standardized Indices/Anomalies (SI/SA) temporal evolution. They are the corresponding temporal evolution of spatial patterns in Fig. 3, from rotated principal component analyses decomposition of SI/SA. Agricultural drought conditions occur when SSI falls below -0.84 , as in Table 2, continuously for at least three months. (Y-axis values are unitless).

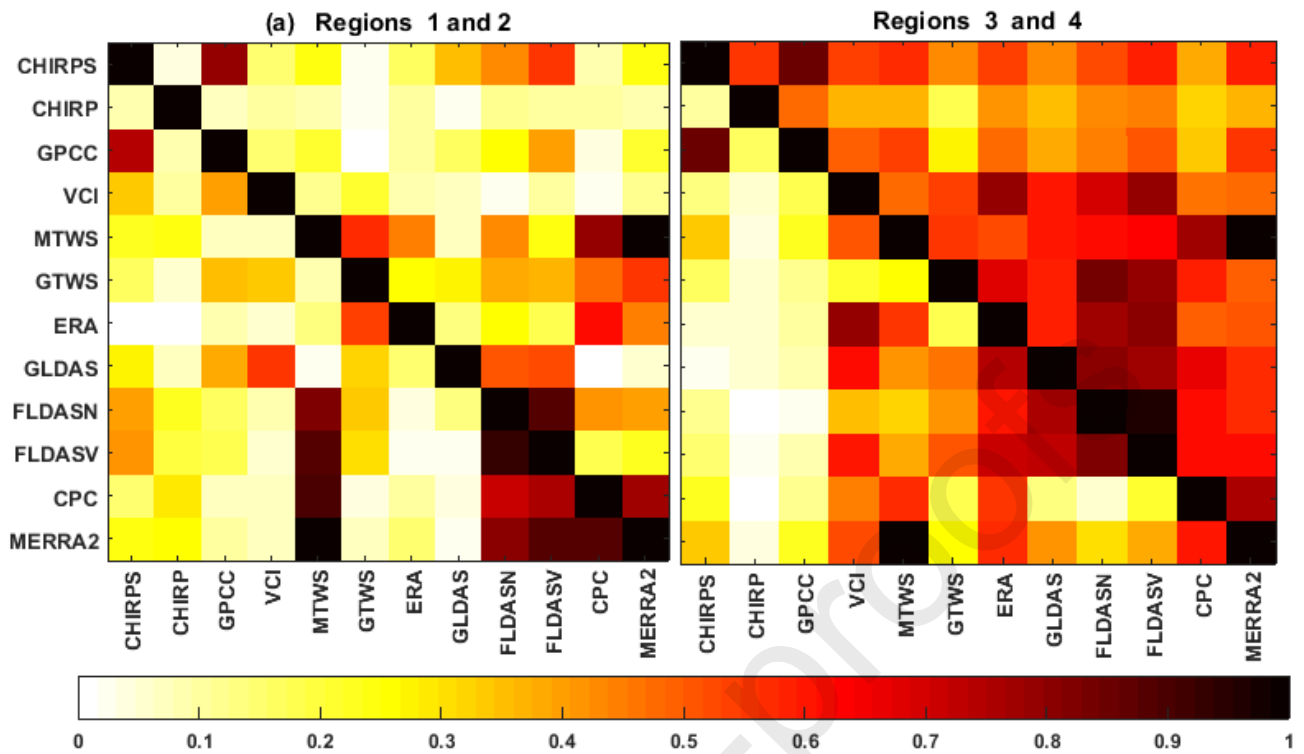


Figure 6: Correlation shaded plot between drought indices by region; (a) upper triangle - Region 1, lower triangle - Region 2; and (b) upper triangle - Region 3, and lower triangle - Region 4. On average, Region 3 has higher correlations while the following products registered high correlation across the region; CHIRPS and GPCC, FLDASN and FLDASV, MTWS and MERRA2, and MTWS and CPC.

403 lyzed through Pearson correlation are shown in Fig. 6. From the correlation coefficients, there
 404 is high degree of consistency across the region between the following products; CHIRPS and
 405 GPCC, FLDASN and FLDASV, MTWS and MERRA2, and MTWS and CPC. In addition,
 406 the majority of the products have on average highest correlations in Region 3 signifying con-
 407 sistent performance. These are consistent with the results outlined above (see Figs. 2, 3,
 408 4, and 5). For the rainfall group, while CHIRPS and GPCC have the lowest correlation in
 409 Region 2, CHIRPS and CHIRP, and GPCC and CHIRP have the lowest correlation in Region
 410 1. However, the soil moisture group do not have any particular region in which the majority
 411 of products had lowest correlations as values varied with product pairs and region.

4.2. Percentage of Areas Under Agricultural Drought and their Consistencies

4.2.1. Consistency of Areas Under Agricultural Drought

In order to analyze the consistency of areas under drought from rainfall and soil moisture products, this section considers the mean differences in areas under drought between various products during 1983 - 1984, 1987, 1999, 2009, and 2010-2011 drought events. These drought events are considered as they had significant impacts on the region (see, e.g., *Elagib and Elhag, 2011*; *Gebrehiwot et al., 2011*; *Masih et al., 2014*; *Viste et al., 2013*). In addition, spatial correlations of the respective Standardized Indices (SPIs and SSIs) during these drought events are used to support the analysis of the mean differences.

Overall, the rainfall products are found to have higher mean differences in the percentage of areas under drought than soil moisture products, i.e., 15.7% vis-a-vis 12.6% at $F(1,2338) = 28.5176$, with $p < 0.0001$. However, the reverse would be true if only gauge based precipitation products (CHIRPS and GPCC) are considered (overall mean percentage difference would be 9.7% as opposed to 15.9%). The larger mean difference is attributed to the inclusion of CHIRP, a satellite only product that seems to have problems capturing the regional precipitation well.

From the rainfall products, the mean differences in percentage of areas under drought due to the gauge density (spatial distribution and temporal availability) is lowest in Ethiopia, followed by South Sudan and Sudan, and highest in Somalia (Fig. 7 a). This is inversely related to the gauge density of both GPCC and CHIRPS (see, Figs. 1d and *Funk et al. (2015)*) and is further supported by relatively high correlation coefficients over Ethiopia vis-à-vis lower coefficients over Somalia (Fig. 7 b). Finally, the mean differences in percentage of areas under drought due to topographical variations are lowest over Somalia (an area of low topographical variation), and highest over South Sudan with Ethiopia and Sudan being in between Fig. 7 a. This is supported by relatively higher correlation coefficients over Somalia compared to the rest of the regions (Fig. 7, c and d)

For the soil moisture products, the mean differences in percentage of areas under drought

439 between various products depend on the products under consideration ($F(3, 1292) = 61.92$,
 440 $p < 0.0001$) and the specific region (country) being considered ($F(3, 1292) = 28$, $p < 0.0001$;
 441 Fig. 8). Different models with similar forcing precipitation translate into lower mean per-
 442 centage difference in areas under drought across the entire region than similar models with
 443 different forcing precipitations (FLDASN-FLDASV vis-a-vis FLDASN-GLDAS; Fig. 8). This
 444 is also reflected by the higher correlation between FLDASN and FLDASV SSIs' compared
 445 to FLDASN and GLDAS SSIs' during the considered drought events (Fig. 8b and e). The
 446 mean difference in the percentage of areas under drought between reanalysis products is lower

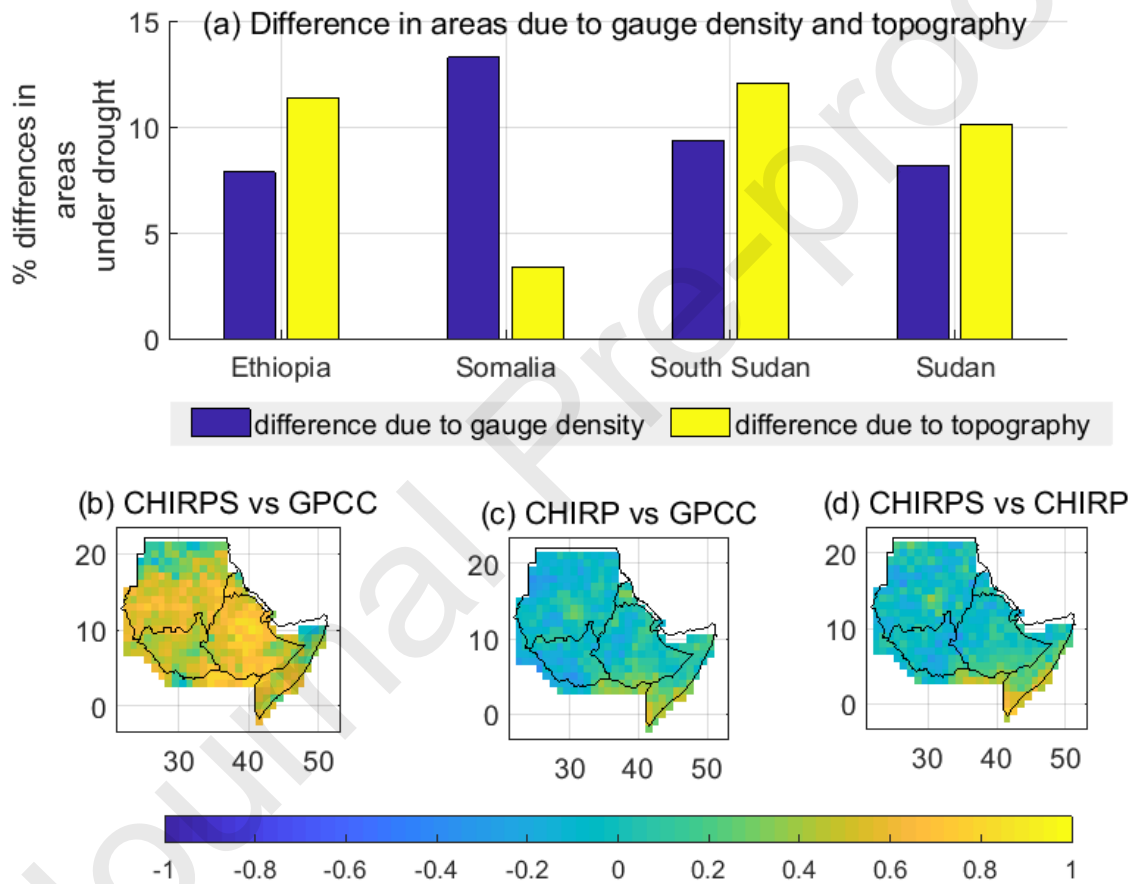


Figure 7: Rainfall products; (a) Mean percentage differences in areas under drought due to gauge density and topography over UGHA, (b) Spatial distribution of SPI correlations for the 1983 - 1984, 1987, 1999, 2009, and 2010-2011 drought events. The correlations are a function of gauge density (b), and topography (c and d).

447 than that between a reanalysis and a normal model product except over Somalia (MERRA-
 448 ERA vis-a-vis FLDASN-MERRA) as also shown by higher correlations between MERRA
 449 and ERA SSI than between FLDASN and MERRA (Fig. 8 a, c and d) during the consid-
 450 ered drought events. The relatively higher difference in mean areas under drought between
 451 MERRA and ERA over Somalia, also reflected by low correlations (Figs. 8 a and d) could
 452 be attributed to the overestimation tendencies of ERA-interim, especially over dry areas as

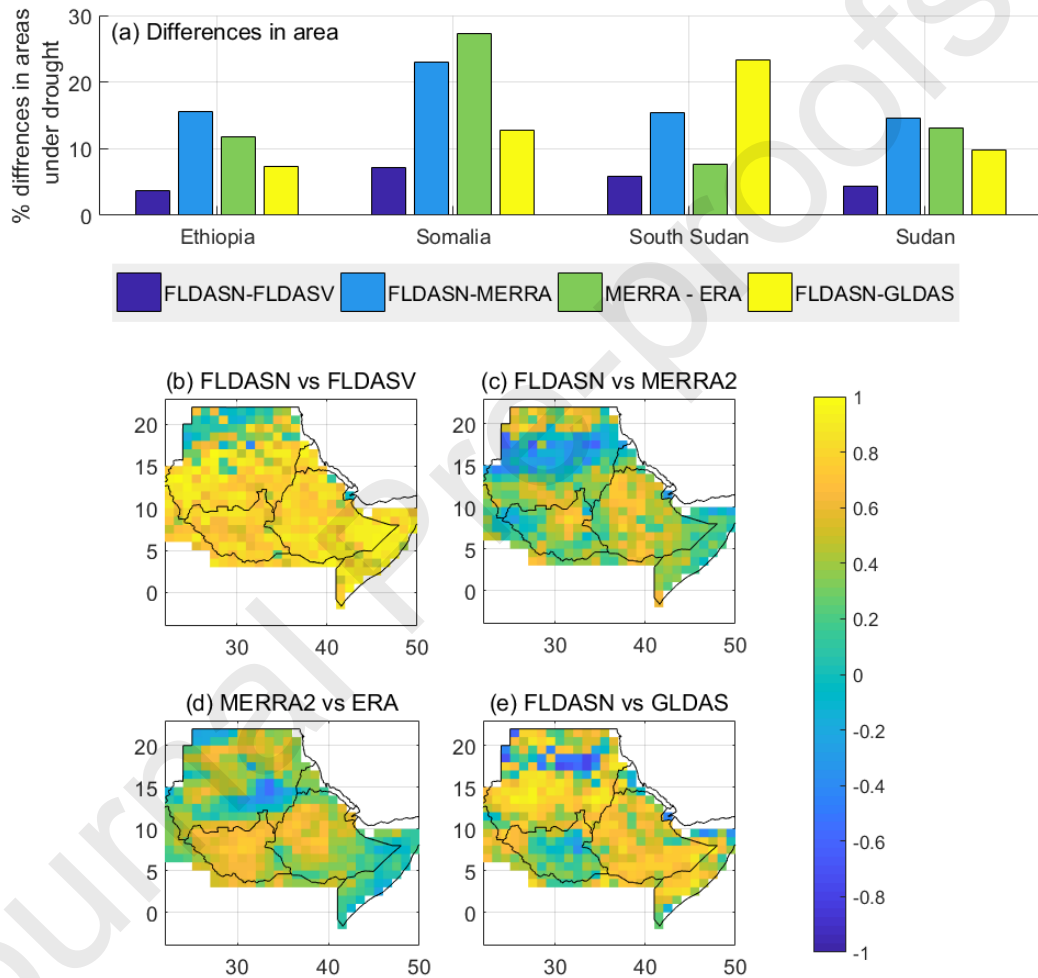


Figure 8: Soil moisture products; (a) Mean percentage differences in areas under drought. Lower mean percentage differences are observed from models forced by same precipitation products (e.g., FLDASN and FLDASV), (b) Spatial distribution of SSI correlations for 1983 - 1984, 1987, 1999, 2009, and 2010-2011 drought events.

453 was shown by *Albergel et al. (2012)*. The differences involving different models with different
 454 forcing precipitation products (FLDASN-MERRA and MERRA-ERA) have the highest mean
 455 difference in the percentage of areas under drought while different models forced with similar
 456 precipitation (FLDASN-FLDASV) have the lowest mean difference in the percentage of areas
 457 under drought across the region. This is supported by higher correlation between FLDASN
 458 and FLDSV SSIs' in comparison to the relatively lower correlations between FLDASN and
 459 MERRA2, and MERRA2 and ERA SSIs' (Fig. 8 b, c, and d). Finally, concerning the regional
 460 variability of the mean percentage differences in areas under drought, Somalia has the highest
 461 mean differences while Ethiopia has the least mean differences on the majority of product
 462 differences considered (Fig. 8 a).

463 *4.2.2. Consistency of Areas Under Different Drought Intensities*

464 In addition to the areas under agricultural drought, it is important to assess the extent
 465 to which each area is affected hence this section analyses the differences in drought intensity
 466 between various products used in section 4.2.1 for the same drought episodes i.e., 1983 - 1984,
 467 1987, 1999, 2009, and 2010-2011 drought events.

468 On average, the mean difference in areas under different drought intensities from rainfall
 469 products is higher than those from soil moisture products when the whole region is considered
 470 in entirety (6.164% vis-a-vis 5.2021% at $F(1, 7018) = 33.91, p < 0.0001$; Figs. 9). The mean
 471 differences in percentage of areas under different drought intensities (moderate, severe, and
 472 extreme) from rainfall products varies with product pairs under consideration ($F(2, 3088) =$
 473 $41.13, p < 0.0001$), the country ($F(3, 3088) = 4.79, p < 0.0001$), and the drought intensity
 474 category ($F(2, 3088) = 91.6, p < 0.0001$) being considered (Fig. 9a-d).

475 For the rainfall products, similar to the case of mean difference in areas under drought
 476 (see, section 4.2.1), the mean difference in percentage of areas under various intensities due
 477 to gauge density is lowest in Ethiopia and highest in Somalia, with Sudan and South Sudan
 478 being in between (Fig. 9 a - d). In addition, the mean difference in percentage of areas under
 479 various drought intensities due to topography is lowest over Somalia and largely the same over

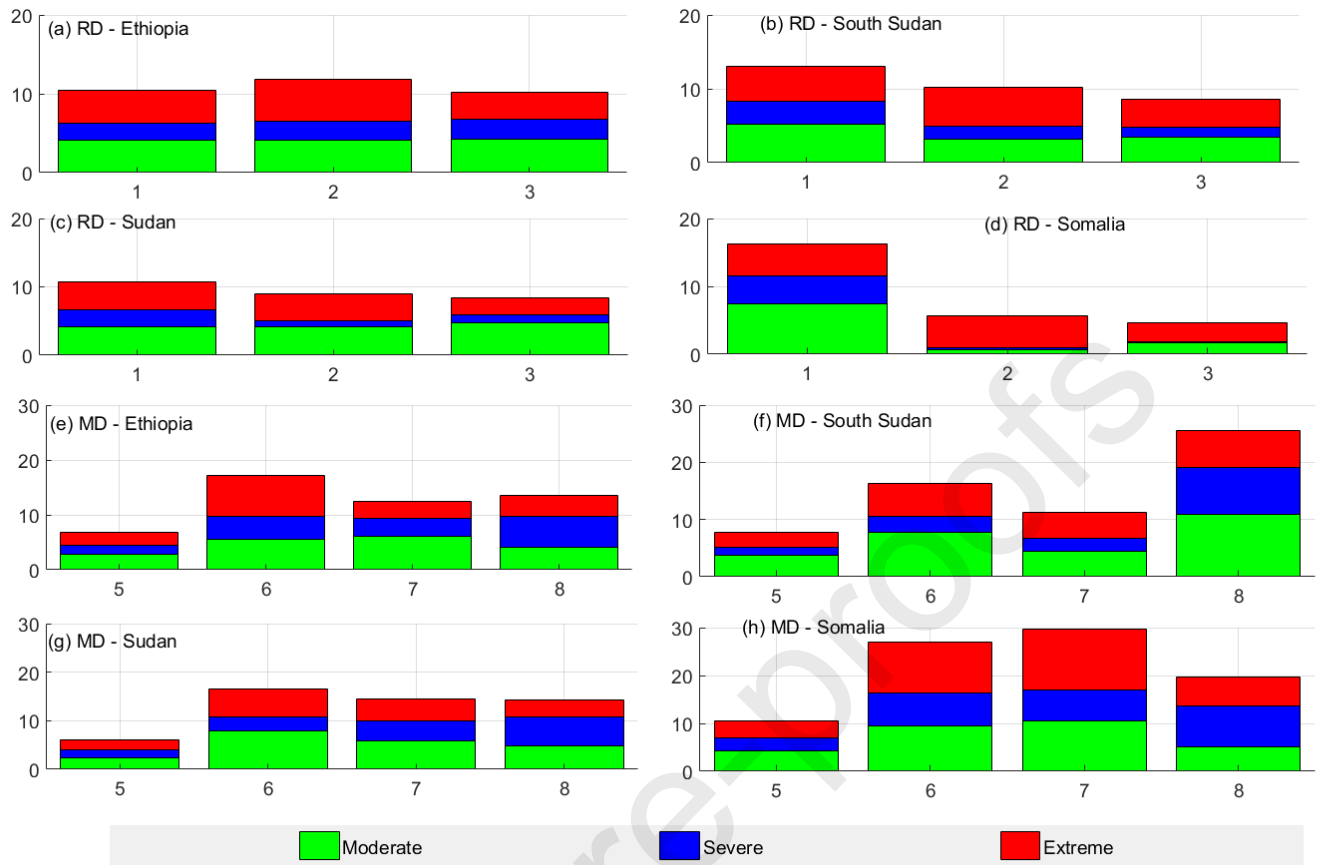


Figure 9: Mean differences in percentage of areas under different drought intensities during 1983 - 1984, 1987, 1999, 2009, and 2010-2011 drought events; (a-d) Rainfall-derived Differences (RD) due to gauge density (1) and topography (2 and 3, are CHIRPS and GPCC derived, respectively), (e-h) Soil moisture-derived differences (MD; 5 = FLDASN - FLDASV, 6 = FLDASN - MERRA2, 7 = MERRA - ERA, and 8= FLDASN - GLDAS. FLDASN - FLDAS NOAH, and FLDASV - FLDAS VIC).

480 the remaining countries (Fig. 9 a - d).

481 Similar to the case of the precipitation products, the mean differences in percentage of areas
 482 under different drought intensities from soil moisture products are dependent on products
 483 pairs ($F(3, 3915) = 77.16, p < 0.0001$), the country ($F(3, 3915) = 49.5, p < 0.0001$), and the
 484 intensity category ($F(2, 3915) = 30.06, p < 0.0001$) under consideration (Fig. 9 e - h). The
 485 mean differences in the percentage of areas under different drought intensities are lower for
 486 FLDASN-FLDASV compared to the rest of the soil moisture pairs across the regions. The

487 mean differences in the percentage of areas under various drought intensities are lowest in
488 Ethiopia and highest over Somalia (Fig. 9 e and h). Like in the case of rainfall products, the
489 mean differences in areas under different drought intensities are lower under severe droughts
490 compared to moderate and extreme, across the countries for all the soil moisture product
491 differences except for FLDASN – GLDAS (5 above). As with the case of differences in the
492 percentage of areas under drought above, similar precipitation forcing with different models
493 contributes to lower differences in intensity information compared to similar models with
494 different forcing precipitations (FLDASN-FLDASV vis-a-vis FLDASN-GLDAS; Fig. 9 e - h).

495 4.3. Effectiveness of Drought Indicators in Capturing Agricultural Drought

496 This section extends the work of *Agutu et al. (2017)*, who evaluated the effectiveness of
497 drought indicators in capturing agricultural drought over East Africa (Kenya, Uganda, and
498 Tanzania), to Ethiopia. Though the rest of the study involved the whole of UGHA, this
499 section is only limited to Ethiopia as Sudan, South Sudan, and Somali carry out both rain-fed
500 and irrigated agriculture (*Elagib and Elhag, 2011; Larsson, 1996*) and therefore their annual
501 crop production does not tally with natural water changes in the environment as represented
502 by the indicators.

503 Both SI (computed using approximately 30 years length of data) and SA (computed using
504 approximately 10 years length of data) are regressed with national annual crop (maize and
505 wheat) production, and the model with least mean prediction error has its proportion of
506 variability explained (R^2) reported (Fig. 10). As in *Agutu et al. (2017)*, SA is necessitated by
507 the need to compare how GTWS performs in relation to other indicators.

508 Based on SI regression with national annual crop production, all the indicators explain
509 over 50% of variability in the national annual crop production (in most instances) except
510 CHIRP and GLDAS (Fig. 10a). These results are largely consistent with those of *Bewket*
511 (2009) and *Funk et al. (2003)* who found a good correlation between crops (teff, wheat, and
512 maize) production and monthly rainfall anomalies over Ethiopia. VCI performs exceptionally
513 well explaining between 67% and 93% of national annual crop production variability. GPCP

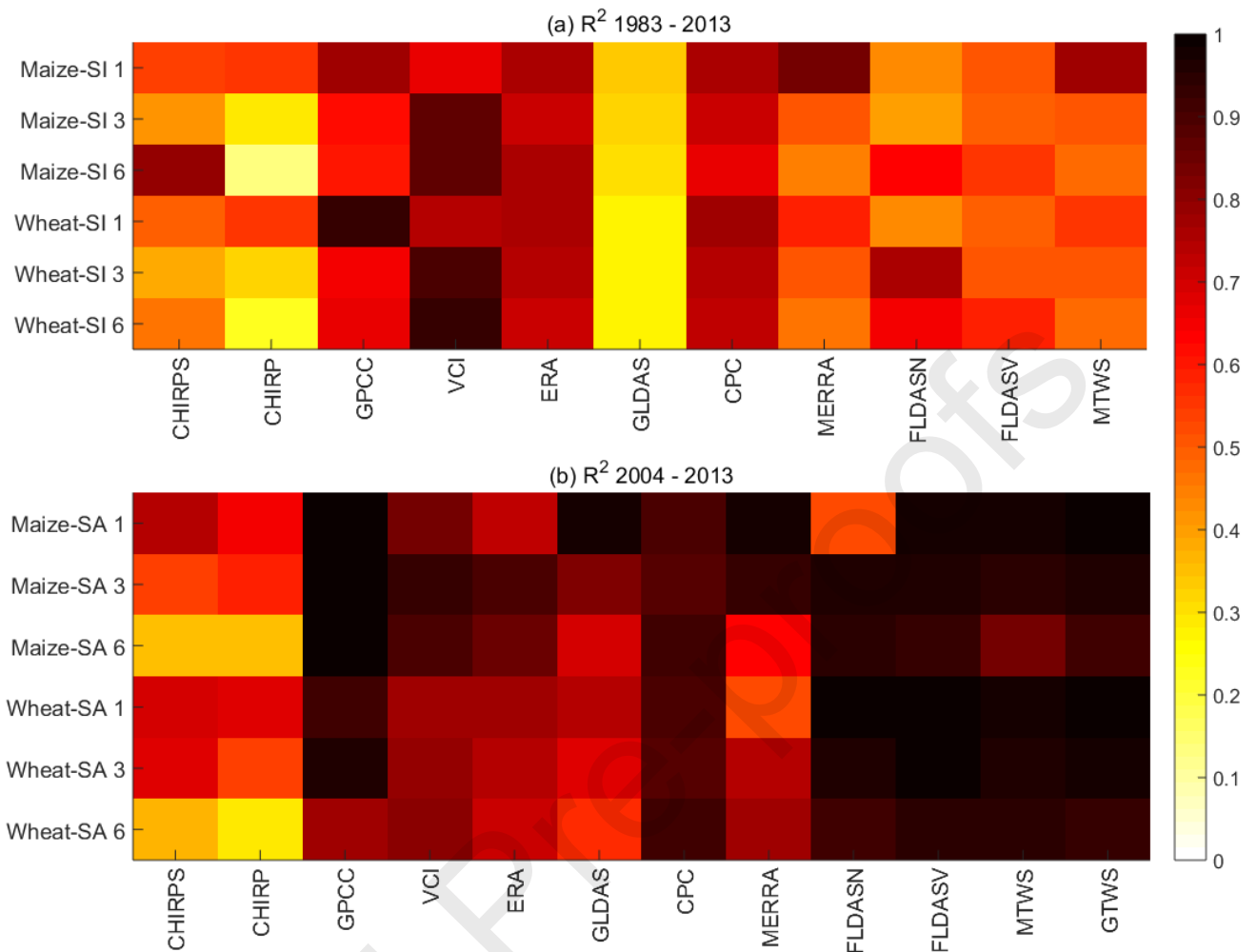


Figure 10: Ethiopian national annual crop (maize and wheat) production variability (R^2) reflected by various drought indices. VCI, GPCC, ERA, CPC, FLDASN, and FLDASV explained relatively higher crop production variabilities, while GLDAS explained lowest variability. The y axis indicates the crop (maize/wheat), SI (for a), and SA (for b) while 1, 3 and 6 indicate the standardization time scales for the indicators on the x axis.

514 explains higher percentage of national annual crop production variability than CHIRPS, which
 515 explains higher variability than CHIRP. In addition, ERA and CPC are seen to perform
 516 better than the rest, FLDASN and FLDASV explains largely equal variabilities while GLDAS
 517 explains the least national annual crop production variability.

518 SA regression generally explains higher annual crop production variabilities than SI (Fig 10b),

519 possibly due to the shorter duration considered. GTWS performs exceptionally well explain-
520 ing between 92% – 99% of the variability in national annual crop production. In addition,
521 FLDASN, FLDASV, CPC, VCI, and GPCC also explain high variabilities. Like in SI regres-
522 sion, GPCC outperformed CHIRPS, which performed better than CHIRP while FLDASN
523 and FLDASV explain almost equal variabilities. Also, FLDASN explain more variability than
524 GLDAS. However, the SA regression results should be interpreted with caution due to the
525 shorter duration of the data considered.

526 The regression results, as pointed out in *Agutu et al. (2017)*, should not be generalized
527 to other areas and time periods since the association of production (yield) with climatic
528 conditions only holds if production factors e.g., areas under cultivation, and farm management
529 practices, remain constant.

530 5. Discussion

531 The spatial patterns of rainfall, VCI, TWS, and majority of the soil moisture products
532 derived drought indicators have been seen to mimic rainfall distribution and/or land cover
533 patterns (Figs. 2 and 3 vis-a-vis Fig. 1b–c) both of which are majorly influenced by to-
534 pographical changes (terrain variations). Topography is a major factor influencing rainfall
535 distribution (see, e.g., *Dinku et al., 2007*; *Romilly and Gebremichael, 2011*; *Dinku et al., 2008*)
536 and to a large extent the land cover classes over the region (*Kurnik et al., 2011*). The spatial
537 variability of soil moisture is closely related to the scales under consideration i.e., at large
538 scales, soil moisture spatial variability is associated with soil types, topography, and vegeta-
539 tion types while at small scales, precipitation and evapotranspiration play major roles (*Huang*
540 *et al., 2012*; *Entin et al., 2000*). This explains the closeness of the majority of the SSI spatial
541 patterns to the land cover classes and/or spatial rainfall distribution (Fig. 3 compared to
542 Fig. 1a–c).

543 Region 3 (southeastern Ethiopia and Somalia) had high consistency in spatial and temporal
544 patterns, largely equal percentage of variabilities explained by rainfall and moisture products,
545 and high average correlation among different products (Figs. 2, 3, 4c, 5c and 6, and Table 4).

546 These could be attributed to relatively flats topography of the region coupled with low rainfall.
547 The combination of flat topography and low rainfall does not seem to give much challenge
548 to the different products in capturing spatio-temporal drought information from the region,
549 hence the high consistency.

550 The variation in the mean differences in percentage of areas under drought due to gauge
551 density was inversely related to the gauge density of both GPCC and CHIRPS (Figs. 7a, 1d,
552 and *Funk et al. (2015)*). The mean percentage differences were lowest over Ethiopia and
553 highest over Somalia (7.9% vis-a-vis 13.3%). Ethiopia has the highest gauge density from both
554 GPCC and CHIRPS while Somalia has the lowest (Figs. 1d, and *Funk et al. (2015)*). Even
555 though GPCC and CHIRPS have in-situ gauge measurements from global historical networks
556 and global teleconnection networks (*Schneider et al., 2014; Funk et al., 2015*), the fluctuation
557 in monthly number of stations available to each (see, e.g., variation in number of available
558 stations for CHIRPS in *Funk et al. (2015)*) is the major source of this difference. In addition,
559 this variation could also be contributed by the additional in-situ stations incorporated in
560 GPCC but absent in CHIRPS (see, *Schneider et al., 2014; Funk et al., 2015*).

561 Other than gauge density, topographical factors were also found to contribute to the mean
562 difference in percentage areas under drought (Figs. 7a and 1a). Somalia had the lowest mean
563 difference in percentage of areas under drought (3.4%) while Ethiopia (11.3%) and South
564 Sudan (12%) had highest mean differences. This could be due to the fact that Somalia with
565 low topographical variation has low influence on how various products characterize rainfall
566 while Ethiopia and South Sudan with rapid changing topography presents difficulty to various
567 products (Fig. 1a). In general, the performance of GPCC is affected by systematic errors
568 (errors associated with systematic gauge-measurements) and sampling errors associated with
569 gauge densities (see, e.g., *Schneider et al., 2014*). The sampling errors are dependent on
570 orography, season and type of rainfall, of which topography plays a large role hence differing
571 performance across the regions. CHIRPS being a combination of satellite-based precipitation
572 and in-situ observations, has its performance dependent on how well the infrared cold cloud

573 duration (CCD) observed precipitation estimates correspond to the actual rainfall and how
574 effective the merging is done, while CHIRP purely depends on CCD (*Funk et al., 2015*).
575 The degree of correspondence between the CCD estimated rainfall and the actual rainfall
576 over a place is influence by topographical factors. It is the topography related difficulties in
577 rainfall representation that translates to mean differences in percentage areas under drought on
578 drought characterization employing these products. Similarly, the influence of gauge density
579 and topographical variations on the mean differences in percentage of areas under different
580 drought intensities (Fig. 9) follows the same logic as above.

581 The closer performance between FLDASN and FLDASV from temporal variability, higher
582 correlations, lower mean differences in percent of areas under drought and different drought
583 intensities, and explained amount of variabilities in crop production (Figs. 5, 8 a, 9 e - h, and
584 10) could be attributed to FLDASN and FLDASV being forced by CHIRPS rainfall. However,
585 they are FLDAS versions driven by different models, Noah and VIC, respectively. Further,
586 their lower mean differences compared to FLDASN and GLDAS, and the higher percentage
587 of variabilities in crop production explained by FLDASN over GLDAS implies that forcing
588 precipitation plays a bigger role in the resulting soil moisture than model difference. This is
589 supported by the fact that both FLDASN and GLDASN are outputs of the same model, Noah,
590 but differing precipitation forcings; FLDASN is forced by CHIRPS while GLDASN is forced
591 by Princeton global meteorological forcing data (see, e.g., *Sheffield et al., 2006; McNally et al.,*
592 *2017*). The role of forcing precipitation in influencing the quality of resulting soil moisture has
593 also been recognized in previous studies (see, e.g., *Dirmeyer et al., 1999, 2004; Entin et al.,*
594 *1999*). In addition, different model characteristics such as different operating soil wetness
595 thresholds, i.e., differing variances and mean values; and critical hydrological thresholds, e.g.,
596 beginning of surface run-off or levels of evaporation at the potential rate (*Dirmeyer et al.,*
597 *2004*), contribute to the differences. Therefore, the largest differences occurred when different
598 models with difference forcing precipitations were considered, e.g., FLDAS and MERRA.

599 Like gauge density based mean differences, the spatial distribution of the moisture mean

600 differences in percentage of areas under drought and different drought intensities were lower
601 over Ethiopia and higher over Somalia (Figs. 8 a and Fig. 9 e - h). However, for the soil
602 moisture products, this could be linked more to the amount of rainfall and/or moisture levels
603 and the individual model thresholds over the region but not directly on topography since
604 Ethiopia has more topography related issues than Somalia (see section 2.1). The influence
605 of topography on the percentage of area differences from soil moisture product is indirectly
606 through the forcing precipitation.

607 The larger mean differences in areas under moderate and extreme droughts than severe
608 droughts observed in all the differences (both rainfall and soil moisture; Figs. 9) across the
609 region could be linked to differences in extreme drought conditions, i.e., lower (moderate) and
610 higher (extreme) as captured by these products. For the soil moisture products, it could be
611 related to the drying thresholds implemented by different models.

612 Unlike in *Agutu et al. (2017)*, over East Africa where CHIRPS performed better than
613 GPCC, here GPCC aided by a higher density of gauge distribution (and CHIRPS impeded by
614 low and high varying number of incorporated in situ stations) explained higher variabilities
615 in national annual crop production. Similar to *Agutu et al. (2017)*, FLDAS explained higher
616 variabilities than GLDAS while MTWS and MERRA2 registered similar performances. The
617 shorter duration regression results explain higher amount of variability in national annual crop
618 production than the long duration probably due to the fact that under the short duration,
619 the factors of production especially the areas under cultivation are constant. The influence
620 of increase in areas under cultivation could be responsible for relatively lower percentage of
621 variabilities explained, see e.g., *Taffesse et al. (2012)* who found a link between the increase
622 in crop production and areas under cultivation over Ethiopia. The relationship between crop
623 production (yields) and moisture availability (climate variables) holds subject to the area
624 under cultivation and production factors (e.g., pesticides, fertilizers, and crop cultivars) being
625 constant.

626 6. Conclusion

627 The study characterized agricultural drought over the upper GHA countries (Ethiopia,
628 Sudan, South Sudan, and Somalia) using rainfall (CHIRPS, CHIRP, and GPCC), mois-
629 ture (ERA-Interim, CPC, GLDAS, FLDAS Noah, FLDAS VIC, and MERRA2), and TWS
630 (MERRA2 and GRACE) products with bias on the influence of topography and gauge density.
631 Further, it considered the consistency of differences in the percentage of areas under drought
632 and different drought intensities from precipitation and selected moisture products. Finally,
633 it evaluated the effectiveness of various drought indicators in explaining agricultural drought
634 over Ethiopia using national annual crop production. The following were the major results:

- 635 (i) The spatial-temporal drought patterns were found to be influenced by topography over
636 the region. All the products were highly consistent over the low land low-medium
637 rainfall regions of Eastern Ethiopian and Somalia while lowest consistency differed across
638 products and regions.
- 639 (ii) The mean differences in percentages of areas under drought (15.87%) and different
640 drought intensities (6.16%) from precipitation products were determined by gauge den-
641 sity (distribution and availability) and topography. The mean differences attributed to
642 gauge density were low in areas of high gauge density (Ethiopia) and higher in areas of
643 low gauge density (Somalia) while the mean differences attributed to topography were
644 low in low varying topographical areas (Somalia) and higher in rapid varying topograph-
645 ical areas (Ethiopia and South Sudan).
- 646 (iii) The mean differences in percentages of areas under drought (12.65%) and different
647 drought intensities (5.20%) from soil moisture products was determined by the dif-
648 ferences in the forcing precipitation, models pairs under consideration, and the regions.
- 649 (iv) In evaluating the utility of various indicators in explaining agricultural drought over
650 Ethiopia, the following were identified as suited for agricultural drought monitoring
651 during the study period; VCI, GPCC, ERA, CPC, and FLDAS (Noah and VIC).

652 The information on the consistency of percentage of areas under drought and different
653 drought intensities is critical in understanding and putting into perspective drought analysis
654 results from different products over the region by various stakeholders. This is important for
655 policy and decision makers as it could inform their decision on the number of people affected
656 and the extent to which they are affected without worrying about particular product, e.g., soil
657 moisture used in any particular analysis. These particular decisions are essential for resource
658 mobilization, aiding mitigation of drought impacts, improving drought response plans and
659 early warning systems, and quantifying drought impacts among others.

Acknowledgments

660

661

662

663

664

665

The authors are grateful to the following organizations for providing the data for this study CSR, FAO, ICGM, NASA, USGS. J.L. Awange would like to thank the financial support of the Alexander von Humboldt Foundation that supported his time at Karlsruhe Institute of Technology. He is grateful to the good working atmosphere provided by his hosts Prof and Hansjörg Kutterer and Prof Bernhard Heck.

Journal Pre-proofs

666

667 **References**

- 668 AghaKouchak, A. (2015), A multivariate approach for persistence-based drought prediction:
669 Application to the 2010–2011 East African Drought, *Journal of Hydrology*, *526*, 127–135,
670 doi:10.1016/j.jhydrol.2014.09.063.
- 671 AghaKouchak, A., N. Nasrollahi, and E. Habib (2009), Accounting for Uncertainties of the
672 TRMM Satellite Estimates, *Remote Sensing*, *1*, 606–619, doi:10.3390/rs1030606.
- 673 Agnew, C., and A. Chappell (1999), Drought in the Sahel, *GeoJournal*, *48*(4), 299–311,
674 doi:10.1023/A:1007059403077.
- 675 Agnew, C. T. (2000), Using the SPI to identify drought, *Drought Network News*, *12*, 6 – 12.
- 676 Agutu, N., J. Awange, A. Zerihun, C. Ndehedehe, M. Kuhn, and Y. Fukuda (2017), Assessing
677 multi-satellite remote sensing, reanalysis, and land surface models' products in character-
678 izing agricultural drought in East Africa, *Remote Sensing of Environment*, *194*, 287 – 302,
679 doi:http://doi.org/10.1016/j.rse.2017.03.041.
- 680 Albergel, C., P. de Rosnay, G. Balsamo, L. Isaksen, and J. Muñoz-Sabater (2012), Soil Mois-
681 ture Analyses at ECMWF: Evaluation Using Global Ground-Based In Situ Observations,
682 *Journal of Hydrometeorology*, *13*(5), 1442–1460, doi:10.1175/JHM-D-11-0107.1.
- 683 Anderson, W. B., B. F. Zaitchik, C. R. hain, M. C. Anderson, M. T. Yilmaz, J. Mecikalski,
684 and L. Schultz (2012), Towards an integrated soil moisture drought monitor for East Africa,
685 *Hydrology and Earth System Sciences*, *16*, 2893–2913, doi:10.5194/hess-16-2893-2012.
- 686 Awange, J., Khandu, M. Schumacher, E. Forootan, and B. Heck (2016), Exploring hydro-
687 meteorological drought patterns over the Greater Horn of Africa (1979–2014) using remote
688 sensing and reanalysis products, *Advances in Water Resources*, *94*, 45 – 59, doi:http://dx.
689 doi.org/10.1016/j.advwatres.2016.04.005.

- 690 Balsamo, G., A. Beljaars, K. Scipal, P. Viterbo, B. van den Hurk, M. Hirschi, and A. K. Betts
691 (2009), A revised hydrology for the ECMWF model: Verification from field site to terrestrial
692 water storage and impact in the integrated forecast system, *Journal of Hydrometeorology*,
693 *10*(3), 623–643, doi:10.1175/2008JHM1068.1.
- 694 Bewket, W. (2009), Rainfall variability and crop production in Ethiopia: Case study in the
695 Amhara region, in *Proceedings of the 16th International Conference of Ethiopian Studies*,
696 vol. 3, edited by S. Ege, H. Aspen, B. Teferra, and S. Bekele, pp. 823–836, Department of
697 Social Anthropology, Norwegian University of Science and Technology, Trondheim.
- 698 Bordi, I., K. Fraedrich, M. Petitta, and A. Sutera (2006), Large-scale assessment of drought
699 variability based on NCEP/NCAR and ERA-40 Re-Analyses, *Water Resources Manage-*
700 *ment*, *20*(6), 899–915, doi:10.1007/s11269-005-9013-z.
- 701 Bosilovich, M., G. Lucchesi, and M. Suarez (2016), MERRA-2: File Spec-
702 ification, *GMAO Office Note No. 9 (Version 1.1)*, 73 pp, available
703 form:http://gmao.gsfc.nasa.gov/pubs/office_notes.
- 704 Bosilovich, M. G., S. Akella, L. Coy, R. Cullather, C. Draper, R. Gelaro, R. Kovach, Q. Liu,
705 A. Molod, P. Norris, W. Chao, R. Reichle, L. Takacs, R. Todling, Y. Vikhliayev, S. Bloom,
706 A. Collon, G. Partyka, S. Firth, G. Labow, S. Pawson, O. Reale, S. Schubert, and M. Suarez
707 (2015), Merra-2: Initial evaluation of the climate, *Technical Report Series on Global Mod-*
708 *eling and Data Assimilation NASA/TM-2015-104606/Vol. 43*, NASA:GSFCG, Available
709 online at <https://gmao.gsfc.nasa.gov/reanalysis/MERRA-2/docs/>.
- 710 Chen, J. L., C. R. Wilson, B. D. Tapley, and J. C. Ries (2004), Low degree gravitational
711 changes from GRACE: Validation and interpretation, *Geophysical Research Letters*, *31*(22),
712 n/a–n/a, doi:10.1029/2004GL021670, 122607.
- 713 Chen, J. L., C. R. Wilson, B. D. Tapley, Z. L. Yang, and G. Y. Niu (2009), 2005 drought event
714 in the Amazon River basin as measured by GRACE and estimated by climate models, *Jour-*

- 715 *nal of Geophysical Research: Solid Earth*, 114(B5), n/a–n/a, doi:10.1029/2008JB006056,
716 b05404.
- 717 Chen, T., R. de Jeu, Y. Liu, G. van der Werf, and A. Dolman (2014), Using satellite based
718 soil moisture to quantify the water driven variability in NDVI: A case study over mainland
719 Australia, *Remote Sensing of Environment*, 140, 330 – 338, doi:http://dx.doi.org/10.1016/
720 j.rse.2013.08.022.
- 721 Damberg, L., and A. AghaKouchak (2014), Global trends and patterns of drought from space,
722 *Theoretical and Applied climatology*, 117, 441–448, doi:10.1007/s00704-013-1019-5.
- 723 Decker, M., M. A. Brunke, Z. Wang, K. Sakaguchi, X. Zeng, and M. G. Bosilovich (2012),
724 Evaluation of the Reanalysis Products from GSFC, NCEP, and ECMWF Using Flux Tower
725 Observations, *Journal of Climate*, 25, 1916–1944, doi:10.1175/JCLI-D-11-00004.1.
- 726 Dee, D. P., S. M. Uppala, A. J. Simmons, P. Berrisford, P. Poli, S. Kobayashi, U. Andrae, M. A.
727 Balmaseda, G. Balsamo, P. Bauer, P. Bechtold, A. C. M. Beljaars, L. van de Berg, J. Bidlot,
728 N. Bormann, C. Delsol, R. Dragani, M. Fuentes, A. J. Geer, L. Haimberger, S. B. Healy,
729 H. Hersbach, E. V. Hólm, L. Isaksen, P. Kállberg, M. Köhler, M. Matricardi, A. P. McNally,
730 B. M. Monge-Sanz, J.-J. Morcrette, B.-K. Park, C. Peubey, P. de Rosnay, C. Tavolato, J.-N.
731 Thépaut, and F. Vitart (2011), The ERA-Interim reanalysis: configuration and performance
732 of the data assimilation system, *Quarterly Journal of the Royal Meteorological Society*,
733 137(656), 553–597, doi:10.1002/qj.828.
- 734 Dinku, T., P. Ceccato, E. Grover-Kopec, M. Lemma, S. J. Connor, and C. F. Ropelewski
735 (2007), Validation of satellite rainfall products over East Africa’s complex topography, *In-*
736 *ternational Journal of Remote Sensing*, 28(7), 1503–1526, doi:10.1080/01431160600954688.
- 737 Dinku, T., S. Chidzambwa, P. Ceccato, S. J. Connor, and C. F. Ropelewski (2008), Validation
738 of high resolution satellite rainfall products over complex terrain, *International Journal of*
739 *Remote Sensing*, 29(14), 4097–4110, doi:10.1080/01431160701772526.

- 740 Dirmeyer, P. A., A. J. Dolman, and N. Sato (1999), The pilot phase of the global soil
741 wetness project, *Bulletin of the American Meteorological Society*, 80(5), 851–878, doi:
742 10.1175/1520-0477(1999)080<0851:TPPOTG>2.0.CO;2.
- 743 Dirmeyer, P. A., Z. Guo, and X. Gao (2004), Comparison, validation, and transferability of
744 eight multiyear global soil wetness products, *Journal of Hydrometeorology*, 5(6), 1011–1033,
745 doi:10.1175/JHM-388.1.
- 746 Dorigo, W., R. de Jeu, D. Chung, R. Parinussa, Y. Liu, W. Wagner, and D. Fernández-
747 Prieto (2012), Evaluating global trends (1988–2010) in harmonized multi-satellite surface
748 soil moisture, *Geophysical Research Letters*, 39(18), doi:10.1029/2012GL052988, 118405.
- 749 Dutra, E., L. Magnusson, F. Wetterhall, H. L. Cloke, G. Balsamo, S. Bousssetta, and F. Pap-
750 penberger (2013), The 2010–2011 drought in the Horn of Africa in ECMWF reanaly-
751 sis and seasonal forecast products, *International Journal of Climatology*, 33, 1720–1729,
752 doi:10.1002/joc.3545.
- 753 Dutra, E., F. Wetterhall, F. Di Giuseppe, G. Naumann, P. Barbosa, J. Vogt, W. Pozzi, and
754 F. Pappenberger (2014), Global meteorological drought - part 1: Probabilistic monitoring,
755 *Hydrology and Earth System Sciences*, 18(7), 2657–2667, doi:10.5194/hess-18-2657-2014.
- 756 Edossa, D. C., M. S. Babel, and A. S. Gupta (2010), Drought analysis in the Awash River
757 Basin, Ethiopia, *Water Resources Management*, 24, 1441–1460, doi:10.1007/s11269-009-
758 9508-0.
- 759 Elagib, N. A. (2013), Meteorological Drought and Crop Yield in Sub-Sahara Sudan, *Interna-
760 tional Journal of Water Resources and Arid Environments*, 2(3), 164–171.
- 761 Elagib, N. A., and M. M. Elhag (2011), Major climate indicators of ongoing drought in Sudan,
762 *Journal of Hydrology*, 409, 612–625, doi:10.1016/j.jhydrol.2011.08.047.

- 763 Entin, J. K., A. Robock, K. Y. Vinnikov, V. Zabelin, S. Liu, A. Namkhai, and T. Adyasuren
764 (1999), Evaluation of global soil wetness project soil moisture simulations, *Journal of the*
765 *Meteorological Society of Japan. Ser. II*, 77(1B), 183–198.
- 766 Entin, J. K., A. Robock, K. Y. Vinnikov, S. E. Hollinger, S. Liu, and A. Namkhai (2000), Tem-
767 poral and spatial scales of observed soil moisture variations in the extratropics, *Journal of*
768 *Geophysical Research: Atmospheres*, 105(D9), 11,865–11,877, doi:10.1029/2000JD900051.
- 769 Fan, Y., and H. van den Dool (2004), Climate Prediction Center global monthly soil mois-
770 ture data set at 0.5° resolution for 1948 to present, *Journal of Geophysical Research*, 109,
771 D10,102, doi:10.1029/2003JD004345.
- 772 Farahmand, A., and A. AghaKouchak (2015), A generalized framework for deriving non-
773 parametric standardized drought indicators, *Advances in Water Resources*, 76, 140 – 145,
774 doi:10.1016/j.advwatres.2014.11.012.
- 775 Forina, M., C. Armanino, S. Lanteri, and R. Leardi (1988), Methods of Varimax Rotation in
776 Factor Analysis with Applications in Clinical and Food Chemistry, *Journal of Chemomet-*
777 *rics*, 3, 115–125, doi:10.1002/cem.1180030504.
- 778 Funk, C., P. Steffen, G. B. Senay, J. Rowland, and J. Verdin (2003), Es-
779 timating Meher crop production using rainfall in the ‘long cycle’ region of
780 Ethiopia, *Special report*, FEWS-NET, USGS/FEWS/USAID. Accessed from:
781 <http://reliefweb.int/sites/reliefweb.int/files/resources> on March 15, 2015.
- 782 Funk, C., A. Hoell, S. Shukla, I. Blade, B. Liebmann, J. B. Roberts, F. R. Robertson, and
783 G. Husak (2014), Predicting East African spring droughts using Pacific and Indian Ocean
784 sea surface temperature indices, *Hydrology and Earth System Sciences*, 18, 4965–4978,
785 doi:10.5194/hess-18-4965-2014.
- 786 Funk, C., P. Peterson, M. Landsfeld, D. Pedreros, J. Verdin, S. Shukla, G. Husak, J. Rowland,
787 L. Harrison, A. Hoell, and J. Michaelsen (2015), The climate hazards infrared precipita-

- 788 tion with stations - a new environmental record for monitoring extremes, *Scientific Data*,
789 2(150066), 1–21, doi:10.1038/sdata.2015.66.
- 790 Gebrehiwot, T., A. van der Veen, and B. Maathuis (2011), Spatial and temporal assessment
791 of drought in the Northern highlands of Ethiopia, *International Journal of Applied Earth
792 Observation and Geoinformation*, 13(3), 309 – 321, doi:10.1016/j.jag.2010.12.002.
- 793 Gedif, B., L. Hadish, S. Addisu, and K. V. Suryabhagavan (2014), Drought risk assessment
794 using remote sensing and gis: the case of southern zone, Tigray Region, Ethiopia, *Journal
795 of natural Science Research*, 4(23), 87–94, ISSN 2225-0921.
- 796 Geladi, P., and B. R. Kowalski (1986), Partial least-squares regression:a tutorial, *Analytica
797 Chemica Acta*, 185, 1 – 17.
- 798 Gringorten, I. I. (1963), A plotting rule for extreme probability paper, *Journal of Geophysical
799 Research*, 68(3), 813–814, doi:10.1029/JZ068i003p00813.
- 800 Guan, K., E. Wood, and K. Caylor (2012), Multi-sensor derivation of regional vegetation
801 fractional cover in Africa, *Remote Sensing of Environment*, 124, 653 – 665, doi:http://dx.
802 doi.org/10.1016/j.rse.2012.06.005.
- 803 Hannachi, A., I. T. Jolliffe, D. B. Stephenson, and N. Trendafilov (2006), In Search of Simple
804 Structures in Climate: Simplifying EOFs, *International Journal of Climatology*, 26, 7–28,
805 doi:10.1002/joc.1243.
- 806 Hochberg, Y., and A. Tamhane (1987), *Multiple comparison procedures*, Wiley series in prob-
807 ability and mathematical statistics: Applied probability and statistics, Wiley.
- 808 Hong, Y., K.-l. Hsu, H. Moradkhani, and S. Sorooshian (2006), Uncertainty quantification
809 of satellite precipitation estimation and monte carlo assessment of the error propaga-
810 tion into hydrologic response, *Water Resources Research*, 42(8), n/a–n/a, doi:10.1029/
811 2005WR004398, w08421.

- 812 Huang, Y., L. Chen, B. Fu, Z. Huang, J. Gong, and X. Lu (2012), Effect of land use and
813 topography on spatial variability of soil moisture in a gully catchment of the Loess Plateau,
814 China, *Ecohydrology*, 5(6), 826–833, doi:10.1002/eco.273.
- 815 Ibrahim, F. (1988), Causes of the famine among the rural population of the Sahelian zone of
816 the Sudan, *GeoJournal*, 17(1), 133–141, doi:10.1007/BF00209083.
- 817 Jennrich, R. I. (1970), Orthogonal Rotation Algorithms, *Psychometrika*, 35(2), 299–235,
818 doi:10.1007/BF02291264.
- 819 Jolliffe, I. T. (1995), Rotation of Principal Components: Choice of normalization constraints,
820 *Journal of Applied Statistics*, 22(1), 29–35, doi:10.1080/757584395.
- 821 Jolliffe, I. T. (2002), *Principal Component Analysis*, Springer Series in Statistics, second ed.,
822 Springer.
- 823 Kaiser, H. F. (1958), The Varimax Criterion for analytic rotation in Factor analysis, *Psy-*
824 *chometrika*, 23(3), 187–200, doi:10.1007/BF02289233.
- 825 Katz, R. W., and M. H. Glantz (1986), Anatomy of a rainfall index, *Monthly Weather Review*,
826 114, 764–771, doi:10.1175/1520-0493(1986)114< 0764 : AOARI >2.0.CO;2.
- 827 King, B. (2010), Analysis of variance, in *International Encyclopedia of Education*, edited by
828 P. Peterson, E. Baker, and B. McGaw, third edition ed., pp. 32 – 36, Elsevier, Oxford,
829 doi:https://doi.org/10.1016/B978-0-08-044894-7.01306-3.
- 830 Kogan, F. (1995), Application of vegetation index and brightness temperature for drought
831 detection, *Advances in Space research*, 15, 91 – 100, doi:10.1016/0273-1177(95)00079-T.
- 832 Kurnik, B., P. Barbosa, and J. Vogt (2011), Testing two different precipitation datasets to
833 compute the standardized precipitation index over the Horn of Africa, *International Journal*
834 *of Remote Sensing*, 32(21), 5947–5964, doi:10.1080/01431161.2010.499380.

- 835 Kutner, M. (2005), *Applied Linear Statistical Models*, McGraw-Hill international edition,
836 McGraw-Hill Irwin.
- 837 Kutzbach, J. E. (1967), Empirical Eigenvector of Sea-Level Pressure, Surface Temperature and
838 Precipitation Complexes over North America, *Journal of Applied Meteorology*, 6, 791–802,
839 doi:10.1175/1520-0450(1967)006 < 0791 : *EEOSLP* > 2.0.CO;2.
- 840 Larsson, H. (1996), Relationship between rainfall and sorghum, millet and sesame in
841 the Kassala Province, Eastern Sudan, *Journal of Arid Environment*, 32(2), 211–223,
842 doi:10.1006/jare.1996.0018.
- 843 Long, D., B. R. Scanlon, L. Longuevergne, A. Y. Sun, D. N. Fernando, and H. Save (2013),
844 GRACE satellite monitoring of large depletion in water storage in response to the 2011
845 drought in Texas, *Geophysical Research Letters*, 40, 3395 – 3401, doi:10.1002/grl.50655.
- 846 Longley, C., R. Jones, M. H. Ahmed, and P. Audi (2001), Supporting local seed systems in
847 southern Somalia: a developmental approach to agricultural rehabilitation in emergency
848 situations, *Network paper 115*, Agricultural Research and Extension Network, 20 pp.
- 849 Lorenz, E. N. (1956), Empirical Orthogonal Function and Statistical Weather Prediction,
850 *Statistical forecasting project: Scientific report no. 1*, Department of Meteorology, MIT,
851 Retrieved from: <http://eaps4.mit.edu/research/Lorenz/>, on March 15, 2015.
- 852 Lough, J. M. (1997), Regional indices of climate variation: temperature and precip-
853 itation in Queensland, Australia, *International Journal of Climatology*, 17, 55–66,
854 doi:10.1002/(SICI)1097-0088(199701)17:1 < 55 :: *AID – JOC109* >3.0.CO;2-Z.
- 855 Lyon, B. (2014), Seasonal Drought in the Greater Horn of Africa and Its Recent Increase
856 during the March–May Long Rains, *Journal of Climate*, 27, 7953–7975, doi:10.1175/JCLI-
857 D-13-00459.1.

- 858 Masih, I., S. Maskey, F. E. F. Mussá, and P. Trambauer (2014), A review of droughts on
859 the African continent: a geospatial and long-term perspective, *Hydrology and Earth System*
860 *Sciences*, 18(9), 3635–3649, doi:10.5194/hess-18-3635-2014.
- 861 McKee, T. B., N. J. Doesken, and J. Kleist (1993), The Relationship of drought frequency and
862 duration to time scale, in *Conference Proceedings*, eighth Conference of Applied Climatology,
863 Anaheim, California.
- 864 McNally, A., S. Shukla, K. R. Arsenault, S. Wang, C. D. Peters-Lidard, and J. P. Verdin
865 (2016), Evaluating ESA CCI soil moisture in East Africa, *International Journal of Applied*
866 *Earth Observation and Geoinformation*, 48, 96 – 109, doi:http://dx.doi.org/10.1016/j.jag.
867 2016.01.001.
- 868 McNally, A., K. Arsenault, S. Kumar, S. Shukla, P. Peterson, S. Wang, C. Funk, C. D.
869 Peters-Lidard, and J. P. Verdin (2017), A land data assimilation system for sub-
870 Saharan Africa food and water security applications, *Scientific Data*, 4(170012), 1–21,
871 doi:10.1038/sdata.2017.12.
- 872 Moore, P., and S. D. P. Williams (2014), Integration of altimetric lake levels and GRACE
873 gravimetry over Africa: Inferences for terrestrial water storage change 2003 – 2011, *Water*
874 *Resource Research*, 50, 9696–9720, doi:10.1002/2014WR015506.
- 875 Naresh Kumar, M., C. S. Murthy, M. V. R. Sesha Sai, and P. S. Roy (2009), On the use
876 of Standardized Precipitation Index (SPI) for drought intensity assessment, *Meteorological*
877 *Applications*, 16(3), 381–389, doi:10.1002/met.136.
- 878 Naumann, G., E. Dutra, F. Pappenberger, F. Wetterhall, and J. V. Vogt (2014), Comparison
879 of drought indicators derived from multiple data sets over Africa, *Hydrology and Earth*
880 *System Sciences*, 18, 1625–1640, doi:10.5194/hess-18-1625-2014.
- 881 Nicholson, S. E. (2014), A detailed look at the recent drought situation in the Greater Horn
882 of Africa, *Journal of Arid Environments*, 103, 71–79, doi:10.1016/j.jaridenv.2013.12.003.

- 883 Olsson, L. (1993), On the causes of famine: drought, desertification and market failure in the
884 Sudan, *Ambio*, 22(6), 395–403, url:<http://www.jstor.org/stable/4314110>.
- 885 Peters, A. J., E. A. Waletr-Shea, L. Ji, A. Viña, M. Hayes, and M. V. Svoboda (2002),
886 Drought monitoring with NDVI-Based Standardized Vegetation Index, *Photogrammetric*
887 *Engineering & Remote Sensing*, 68, 71 – 75.
- 888 Pinzon, J. E., and C. J. Tucker (2014), A Non-Stationary 1981–2012 AVHRR NDVI3g Time
889 Series, *Remote Sensing*, 6(8), 6929, doi:10.3390/rs6086929.
- 890 Preisendorfer, R. W. (1988), *Principal Component Analysis in Meteorology and Oceanography*,
891 Development in Atmospheric Science 17, Elsevier, Elsevier, Amsterdam .
- 892 Pricope, N. G., G. Husak, D. Lopez-Carr, C. Funk, and J. Michaelsen (2013), The climate-
893 population nexus in the East African Horn: Emerging degradation trends in rangeland
894 and pastoral livelihood zones, *Global Environmental Change*, 23(6), 1525 – 1541, doi:<http://dx.doi.org/10.1016/j.gloenvcha.2013.10.002>.
- 896 Quiring, S. M. (2009), Developing objective operational definitions for monitoring
897 drought, *Journal of Applied Meteorology and Climatology*, 48(6), 1217–1229, doi:10.1175/
898 2009JAMC2088.1.
- 899 Quiring, S. M., and S. Ganesh (2010), Evaluation of utility of Vegetation Condition Index
900 (VCI) for monitoring meteorological drought in Texas, *Agriculture and Forest Meteorology*,
901 150, 330 – 339, doi:10.1016/j.agrformet.2009.11.015.
- 902 Raziei, T., B. saghajian, A. A. Paulo, L. S. Pereira, and I. Bordi (2009), Spatial patterns and
903 temporal variability of drought in Western Iran, *Water Resource Management*, 23, 439–455,
904 doi:10.1007/s11269-008-9282-4.
- 905 Reichle, R. (2012), *The MERRA -Land Data Product*, Global Modelling and Assimilation
906 Office, version 1.0 ed., <http://gmao.gsfc.nasa.gov>.

- 907 Rienecker, M. M., M. J. Suarez, R. Gelaro, R. Todling, J. Bacmeister, E. Liu, M. G. Bosilovich,
908 S. D. Schubert, L. Takacs, G.-K. Kim, S. Bloom, J. Chen, D. Collins, A. Conaty, A. da Silva,
909 W. Gu, J. Joiner, R. D. Koster, R. Lucchesi, A. Molod, T. Owens, S. Pawson, P. Pegion,
910 C. R. Redder, R. Reichle, F. R. Robertson, A. G. Ruddick, M. Sienkiewicz, and J. Woollen
911 (2011), MERRA: NASA's Modern-Era Retrospective Analysis for Research and Applica-
912 tions, *Journal of Climate*, *24*(14), 3624–3648, doi:10.1175/JCLI-D-11-00015.1.
- 913 Rodell, M., P. R. Houser, U. Jambor, J. Gottschalck, K. Mitchell, C. J. Meng, K. Arse-
914 nault, B. Cosgrove, J. Radakovich, M. Bosilovich, J. K. Entin, J. P. Walker, D. Lohmann,
915 and D. Toll (2004), The Global Land Data Assimilation System, *Bulletin of the American*
916 *Meteorological Society*, *85*(3), 381 – 394, doi:10.1175/BAMS-85-3-381.
- 917 Rojas, O., A. Vrieling, and F. Rembold (2011), Assessing the drought probability for agri-
918 cultural areas in Africa with coarse resolution remote sensing imagery, *Remote Sensing of*
919 *Environment*, *115*, 343 – 352, doi:10.1016/j.rse.2010.09.006.
- 920 Romilly, T. G., and M. Gebremichael (2011), Evaluation of satellite rainfall estimates over
921 Ethiopian river basins, *Hydrology and Earth System Sciences*, *15*(5), 1505–1514, doi:10.
922 5194/hess-15-1505-2011.
- 923 Rouault, M., and Y. Richard (2003), Intensity and spatial extension of drought in South
924 Africa at different time scales, *Water SA*, *29*(4), 489–500, doi:10.4314/wsa.v29i4.5057.
- 925 Rui, H., and A. McNally (2016), FEWS NET Land Data Assimilation System Ver-
926 sion 1 (FLDAS-1) Products README, *NASA/GSFC/HSL*, pp. 1–18, Retrieved from:
927 ftp://hydro1.sci.gsfc.nasa.gov/data/s4pa/FLDAS/FLDAS, On September 23 2016.
- 928 Santos, J. F., I. Pulido-Calvo, and M. M. Portela (2010), Spatial and temporal vari-
929 ability of drought in Portugal, *Water Resource Research*, *46*(3), n/a–n/a, doi:10.1029/
930 2009WR008071, w03503.

- 931 Schneider, U., A. Becker, P. Finger, A. Meyer-Christoffer, M. Ziese, and B. Rudolf (2014),
932 GPCC's new land surface precipitation climatology based on quality-controlled in situ data
933 and its role in quantifying the global water cycle, *Theoretical and Applied Climatology*,
934 *115*(1), 15–40, doi:10.1007/s00704-013-0860-x.
- 935 Sheffield, J., and E. F. Wood (2008), Global trends and variability in soil moisture and drought
936 characteristics, 1950 – 2000, from observation-driven simulations of the terrestrial hydrologic
937 cycle, *Journal of Climate*, *21*(3), 432–458.
- 938 Sheffield, J., G. Goteti, and E. F. Wood (2006), Development of a 50-year high-resolution
939 global dataset of meteorological forcings for land surface modeling, *Journal of Climate*,
940 *19*(13), 3088–3111, doi:10.1175/JCLI3790.1.
- 941 Shukla, S., A. McNally, G. Husak, and C. Funk (2014), A seasonal agricultural drought forecast
942 system for food-insecure regions of East Africa, *Hydrology and Earth System Sciences*,
943 *18*(10), 3907–3921, doi:10.5194/hess-18-3907-2014.
- 944 Sigdel, M., and M. Ikeda (2010), Spatial and temporal analysis of drought in Nepal using stan-
945 dardised precipitation index and its relationship with climate indices, *Journal of Hydrology*
946 *and Meteorology*, *7*(1), 59–74, doi:10.3126/jhm.v7i1.5617.
- 947 Svoboda, M., M. Hayes, and D. Wood (2012), *Standardized precipitation index user*
948 *guide*, World meteorological organization, WMO - No. 1090, Geneva, Accessed from:
949 <http://www.wamis.org/agm/pubs/SPI> on March 15, 2015.
- 950 Taffesse, A. S., P. A. Dorosh, and S. Asrat (2012), Crop production in Ethiopia: regional
951 patterns and trends, *Research Note 11*, International Food Policy Research Institute, Ad-
952 dis Ababa, Ethiopia, Accessed from: [http://www.ifpri.org/publication/crop-production-](http://www.ifpri.org/publication/crop-production-ethiopia-regional-patterns-and-trends)
953 [ethiopia-regional-patterns-and-trends](http://www.ifpri.org/publication/crop-production-ethiopia-regional-patterns-and-trends) on March 15, 2015.
- 954 Tapley, B., S. Belabour, M. Watkins, and C. Reigber (2004), The Gravity Recovery and

- 955 Climate Experiment: Mission overview and early results, *Geophysical Research Letters*, 31,
956 1 – 4, doi:10.1029/2004GL019920.
- 957 Toothaker, L. (1993), *Multiple Comparison Procedures*, no. 89 in Multiple Comparison Pro-
958 cedures, SAGE Publications.
- 959 Tucker, C., J. Pinzon, M. Brown, D. Slayback, E. Pak, R. Mahoney, E. Vermote, and N. El Sa-
960 leous (2005), An extended AVHRR 8-km NDVI dataset compatible with MODIS and
961 SPOT vegetation NDVI data, *International Journal of Remote Sensing*, 26(20), 4485–4498,
962 doi:10.1080/01431160500168686.
- 963 van den Dool, H., J. Huang, and Y. Fan (2003), Performance and analysis of the con-
964 structed analogue method applied to U.S. soil moisture over 1981–2001, *Journal of Climate*,
965 108(D16), 8617, doi:10.1029/2002JD003114.
- 966 Verdin, J., C. Funk, G. Senay, and R. Choularton (2005), Climate science and famine early
967 warning, *Philosophical Transactions of the Royal Society of London B: Biological Sciences*,
968 360(1463), 2155–2168, doi:10.1098/rstb.2005.1754.
- 969 Viste, E., D. Korecha, and A. Sorteberg (2013), Recent drought and precipitation tendencies
970 in Ethiopia, *Theoretical Applied Climatology*, 112, 535–551, doi:10.1007/s00704-012-0746-3.
- 971 von Storch, H., and F. W. Zwiers (1999), *Statistical Analysis in Climate Research*, Cambridge
972 University Press: Cambridge.
- 973 Wahr, J., M. Molenaar, and F. Bryan (1998), Time variability of the Earth’s gravity field:
974 Hydrological and Oceanic effects and their possible detection using GRACE, *Journal of*
975 *Geophysical Research-Solid Earth*, 103(B12), 30,205–30,229, doi:10.1029/98JB02844.
- 976 Wilks, D. S. (2006), *Statistical methods in atmospheric sciences*, second ed., Academic press,
977 Amsterdam.

- 978 Williams, A. P., and C. Funk (2011), A westward extension of the warm pool leads to a
979 westward extension of the Walker circulation, drying Eastern Africa, *Climate Dynamics*,
980 *37*(11), 2417–2435, doi:10.1007/s00382-010-0984-y.
- 981 Wold, S., M. Sjöström, and L. Eriksson (2001), Pls-regression: a basic tool of chemometrics,
982 *Chemometrics and Intelligent Laboratory Systems*, *58*(2), 109 – 130, doi:http://dx.doi.org/
983 10.1016/S0169-7439(01)00155-1.
- 984 Wouters, B., J. A. Bonin, D. P. Chambers, R. E. M. Riva, I. Sasgen, and J. Wahr (2014),
985 GRACE, time-varying gravity, earth system dynamics and climate change, *Reports on*
986 *Progress in Physics*, *77*, 41pp, doi:10.1088/0034-4885/77/11/116801.
- 987 Wu, H., M. J. Hayes, A. Weiss, and Q. Hu (2001), An evaluation of the standardized pre-
988 cipitation index, the China-Z index and the statistical Z-Score, *International Journal of*
989 *Climatology*, *21*, 745–758, doi:10.1002/joc.658.
- 990 Yang, Y., D. Long, H. Guan, B. R. Scanlon, C. T. Simmons, L. Jiang, and X. Xu (2014),
991 GRACE satellite observed hydrological controls on interannual and seasonal variability in
992 surface greenness over mainland Australia, *Journal of Geophysical Research: Biogeosciences*,
993 *119*, 2245–2260, doi:10.1002/2014JG002670.
- 994 Yilmaz, M. T., M. C. Anderson, B. Zaitchik, C. R. Hain, W. T. Crow, M. Ozdogan, J. A.
995 Chun, and J. Evans (2014), Comparison of prognostic and diagnostic surface flux modeling
996 approaches over the Nile River basin, *Water Resources Research*, *50*(1), 386–408, doi:10.
997 1002/2013WR014194.
- 998 Ziese, M., U. Schneider, A. Meyer-Christoffer, K. Schamm, J. Vido, P. Finger, P. Bissolli,
999 S. Pietzsch, and A. Becker (2014), The GPCC drought index – a new, combined and
1000 gridded global drought index, *Earth System Science Data*, *6*(2), 285–295, doi:10.5194/
1001 essd-6-285-2014.